Deep–Sea Research II 173 (2020) 104708

Contents lists available at ScienceDirect

Deep-Sea Research Part II

journal homepage: http://www.elsevier.com/locate/dsr2

DNA metabarcoding reveals organisms contributing to particulate matter flux to abyssal depths in the North East Pacific ocean

Christina M. Preston [a,*,1], Colleen A. Durkin [b,1], Kevan M. Yamahara [a]

[a] Monterey Bay Aquarium Research Institute, 7700 Sandholdt Road, Moss Landing, CA, 95039, USA
[b] Moss Landing Marine Laboratories, 8272 Moss Landing Road, Moss Landing, CA, 95039, USA

ARTICLE INFO

Keywords:
Sinking POM
High flux event
Diatom bloom
Particle-associated communities
Amplicon sequencing
Sediment trap

ABSTRACT

The sequestration of carbon in the deep ocean relies on the export of sinking particulate organic matter (POM) originating in the surface waters and its attenuation by organisms that reprocess and repackage it. Despite decades of research, predicting the variability of POM to the deep ocean remains difficult as there is still a gap in the knowledge as to which and how organisms control or influence POM export. Here, we used DNA metabarcoding of the 16S and 18S rRNA genes to investigate the community in sinking particulates collected over 9-months (November 2016–July 2017) at Station M, located within the California Current ecosystem. Particle-associated communities were collected in sediment traps (3900 m and 3950 m), in aggregates that settled on the sea floor (4000 m), and in seawater from the overlying water column. For a majority of the deployment, particulate organic carbon (POC) fluxes were within the Station M long-term time series mean ± σ (8.3 ± 7.9 mg C m^{-2} d^{-1}). In late June, a high flux event (>long-term POC mean+2σ) was captured, accounting for 44% of the POC collected during the study. The rRNA genes within the sinking particles indicated highly variable eukaryal communities over time, including the export of oligotrophic autotrophs likely by various metazoan taxa during winter, the sporadic and dominant presence of diverse radiolarian orders, and the important role of coastal diatoms during seasonal increases in POC flux. Specifically, the onset of the high POC flux event in June was attributed to the export of a single coastal diatom species. A coincident increase in the relative abundance of metazoan sequences suggests that zooplankton grazing on the diatom community played a role in rapid transport of large quantities of POC to the deep sea. Analysis of the 16S rRNA gene community supported the presence of highly processed POM during winter due to the high relative abundance of deep sea Gammaproteobacteria, that transitioned to fresher, more labile POM with the arrival of a diatom bloom community. These observations support long standing paradigms of particulate export to the deep sea, including its origin and mechanisms of export mediated by a diverse community of organisms, and implicate rapidly exported diatom blooms as at least one source of the increasingly frequent episodic flux events that account for most POC sequestered in the deep ocean at Station M.

1. Introduction

Surface and abyssal ocean ecosystems are separated by thousands of meters of water but are strongly connected by the sinking of particulate organic matter (POM) (Conte et al., 2001; Lampitt et al., 2010; Smith et al., 2013, 2006; 2008; Wilson et al., 2013; Wong et al., 1999). The majority of POM that reaches the sea floor originates in the surface ocean (Ducklow et al., 2001; Turner, 2015), where the potential magnitude of POM export is largely set by surface phytoplankton production (for review see Herndl and Reinthaler, 2013). Particles undergo numerous transformations during their descent from degradation by microbes (Cho and Azam, 1988; DeLong et al., 1993; Fontanez et al., 2015; Nagata et al., 2010; Smith et al., 1992) to grazing and repackaging into fecal pellets by heterotrophic grazers (Belcher et al., 2019; Caron et al., 1989; Ducklow et al., 2001; Lampitt et al., 2010; Lampitt, 1992; Schnetzer, 2002; Steinberg et al., 2012, 2002; Stone and Steinberg, 2016; Turner, 2015; Wilson and Steinberg, 2010) and transport via pelagic organisms (Hansen et al., 1996; Katija et al., 2017; Lebrato et al., 2013; Robison et al., 2005; Smith et al., 2014; Steinberg and Landry, 2017). POM escaping the upper ocean through sinking provides energy

* Corresponding author.
E-mail address: preston@mbari.org (C.M. Preston).
[1] These authors contributed equally to this work.

https://doi.org/10.1016/j.dsr2.2019.104708
Received 24 August 2019; Received in revised form 6 December 2019; Accepted 12 December 2019
Available online 24 December 2019

and nutrients to abyssal ecosystems and plays a key role in the global carbon cycle by transporting carbon out of the surface ocean and sequestering it at depth.

The quantity and quality of particles that reach abyssal depths is highly variable. Some of the variation is likely due to seasonality, geography, and vertical distribution of organisms within the water column that both produce POC and mediate its transformation (Alldredge and Silver, 1988; Francois et al., 2002; Henson et al., 2012; Riley et al., 2012). In addition, POC export is dependent on the sinking rates of different types of particulates including marine snow (>0.5 mm), fecal pellets, phytodetritus, and rare, but large "dragon king" particles (Bochdansky et al., 2016; Buesseler et al., 2008; De La Rocha and Passow, 2007; Turner, 2015). Resolving the organismal composition within different types of sinking particles has the potential to identify both the ecological source and biological transformations that determine the quantity and quality of POM delivery to the sea floor.

Organismal composition within sinking particles has been evaluated through the physical description of particulates collected in sediment traps, for example enumeration of different sources of fecal pellets (Silver and Gowing, 1991; Wilson et al., 2013) or identification of visible and intact phytoplankton cells (Beaulieu and Smith, 1998; Durkin et al., 2016; Ebersbach et al., 2014; Rynearson et al., 2013; Silver and Bruland, 1981; Silver and Gowing, 1991; Waite et al., 1992). These observations have been essential in identifying processes that affect sinking rates or how particular phytoplankton assemblages contribute to the biological carbon pump. However, these approaches can only resolve visible and intact particles and cells, while overlooking small microbes with ambiguous morphologies or organismal remains that cannot be distinguished within sinking detritus. Thus, important contributors that mediate POM entry into the biological pump may be missed by traditional microscopy observations.

Recent studies have identified the origin, processing, and sinking mechanisms of POM through the nucleic acid signatures collected either by fractionation of water column samples or within sediment traps (Amacher et al., 2013, 2009; Boeuf et al., 2019; Eloe et al., 2011; Fontanez et al., 2015; Guidi et al., 2016; Gutierrez-Rodriguez et al., 2019; Mestre et al., 2018; Xu et al., 2018). Even with caveats of using sequence data to infer community structure (Biard et al., 2017; Caron and Hu, 2019; Kembel et al., 2012; Lin, 2011), these recent studies suggest that genetic approaches are useful for identifying influential ecological pathways of carbon export. For example, both sequence data and physical observations have identified rhizaria as major global contributors to POM export near the surface and to abyssal depths (Amacher et al., 2009; Biard et al., 2016; Decelle et al., 2013; Gutierrez-Rodriguez et al., 2019; Lampitt et al., 2009; Stukel et al., 2018a). It is still unknown how different taxa (e.g. diatom, radiolarian, or metazoan) impact the amount or quality of the POC reaching long-term sequestration depths and how those taxa affect weekly, seasonal, or annual variation in carbon export.

Since 1989, the deep ocean ecosystem has been studied at Station M (35° 08.7975′ N Latitude, 122° 58.4328′ W Longitude, 4000 m deep), generating long-term observations of particulate carbon fluxes collected in sediment traps (Smith and Druffel, 1998). Due to its location within the California Current ecosystem, Station M has high seasonality in phytoplankton blooms and is influenced by both coastal and offshore processes. Particulate carbon flux is at its lowest in the winter months, increases in the spring, and remains elevated through the early fall. The seasonal cycle of carbon flux is punctuated by short duration, high magnitude flux events typically occurring between the spring and fall months. These episodic events can provide up to one half of the year's particulate organic carbon (POC) flux to the ocean sea floor communities (Smith et al., 2018), but it is still unclear as to what organisms cause these events. Episodic flux events have been observed more frequently in recent years, driving a long-term increase in the measured POC flux at Station M (Smith et al., 2018).

We used a combination of sampling methods (sediment traps, water column, and sea floor aggregate samples) to investigate the diversity of organisms that contribute to the seasonal cycle of POM flux observed at Station M from November 2016 to July 2017. Within the sediment trap time series, we captured the beginning of the 2017 summer POC flux event (Smith et al., 2018). The small subunit rRNA gene diversity (18S and 16S) determined from meta-barcoded amplicons was used to compare the different sampling methods and to identify genetic signatures of organisms within sinking particulates over time, that contribute to and affect the attenuation of POM during average and high POC fluxes.

2. Methods

2.1. Collection of particulates in sediment traps

Two McLane sediment traps (East Falmouth, MA, USA) were deployed on a single mooring at Station M to collect sinking particulates at 50 m above bottom (mab) and 100 mab from November 11, 2016 to March 23, 2017 and again from March 25 to July 23, 2017. Each sediment trap carried 20 sample bottles. Ten of the sample bottles on each trap were deployed with 250 ml of 0.1 μm filtered RNA-stabilizing buffer (density ~1.2 g ml^{-1}, De Wit et al., 2012) for nucleic acid preservation. These were interleaved with collection bottles containing a different fixative and open for only 2 h. Data from the other collection bottles were not presented in this study. A time series of 25 total samples were collected serially across two depths and over two deployments. Each bottle collected ~10.9 days of sinking POM. During the initial deployment, sample bottles were open at 50 mab from Nov. 11 to Jan. 16 and at 100 mab from Dec. 14 to March 21. Sample bottles from the first deployment were recovered March 24 and the trap was redeployed. Samples were collected at 50 mab March 25-July 2 and at 100 mab July 13–23. Only during the first deployment, from December 14 to January 16, were sediment traps open at 50 mab and 100 mab at the same time; an overlap of three sample points. Upon recovery, nucleic acid traps were stored at 4 °C until processing. Zooplankton floating at the top of the sample bottle and the majority of the overlying RNA later were removed prior to subsampling. The volume remaining in the trap bottles was estimated prior to mixing and subsampling. Trap bottles were subsampled in triplicate (0.5 ml) using a wide tip pipet (5 mm ID) and collected onto 0.2 μm filters (GSWP, MilliporeSigma, Darmstadt, Germany) using vacuum filtration. This method of subsampling selected against larger organisms (e.g. pyrosomes) within the collected particulate material. Filters were stored at −80 °C until nucleic acid extraction.

POC and mass flux measurements were made from POM collected in a separate, co-deployed sediment trap array at 50 mab containing formaldehyde. Detailed collection and analysis methods are provided in Smith et al. (2018). Briefly, cups were prefilled with 5% formaldehyde prior to deployment. Each cup was open for 10 days from November 15, 2016–March 24, 2017 and 11 days from March 27-August 6, 2017. Upon collection, zooplankton were removed, and samples were freeze-dried, and analyzed for total and inorganic carbon content from which organic carbon was calculated (Smith et al., 2014). The twenty-two integrated trap samples were used to estimate the daily mass and POC fluxes. Because the formaldehyde containing trap was programed to a different sampling schedule than the trap designated for nucleic acid sampling, the daily fluxes corresponding to the collection dates of the nucleic acid traps were averaged to determine the POC and mass flux per sample. These data were compared to variation in community composition as determined by the sequence data.

A high-resolution camera and a fluorescence imaging system mounted on the Benthic Rover (Sherman and Smith, 2009) were used to estimate sea floor detrital aggregate coverage and sediment-surface fluorescence resulting from chlorophyll excitation as previously described (Smith et al., 2014).

2.2. Water column sampling

During servicing of sediment traps at Station M, November 10–11 2016 and March 23–25 2017, eight water column samples (200 m, oxygen minimum ~700 m, 1000 m, 2000 m, 3000 m, 3350 m, 3900 m, and 3960 m) were collected in 5 L Niskin bottles during multiple dives of a remotely operated vehicle (ROV). Upon recovery of the ROV, seawater samples in Niskin bottles were drained into acid washed (10% hydrochloric acid) and autoclaved polypropylene carboys. We used serial filtration to selectively enrich for particle-associated and free-living organisms. Particulates in each seawater sample (approximately 3.5 L) were fractionated (>5 μm and 5 μm–0.2 μm) using separate inline filter holders (Avantec, Dublin, CA) containing 5 μm or 0.2 μm filters (PVDF, Millipore-Sigma) with peristaltic filtration (Masterflex L/S Series peristaltic pump, Cole Parmer, Vernon Hills, IL). Residual seawater was evacuated using a 10 cc syringe and filters were immediately frozen and stored at −80 °C until processed.

2.3. Sea floor aggregate sampling

Many detrital aggregates (Supp. Fig. 1) were observed on the sea floor at Station M in March 2017, which we presume had arrived as sinking POM prior to our occupation of the site. Five representative aggregates were collected by the ROV using push cores on March 25 and 26, 2017. Upon recovery of the ROV, sea floor aggregates along with minimal volume (<1 ml) of overlaying sediment seawater were removed using a plastic pipette with an opening of approximately 5 mm diameter. Samples were frozen at −80 °C in cryovials until processed.

2.4. Nucleic acid extraction

Nucleic acids were extracted from filters containing particulates collected by sediment traps and by filter-fractionated water column samples using AllPrep PowerViral DNA/RNA Kit (Qiagen, Hilden, Germany). Sample filters containing beads and lysis buffer with beta mercaptoethanol (700 μl) were mechanically homogenized in a mini beadbeater (BioSpec, Bartlesville, OK) for 2 min using the Qiagen supplied bead tubes. The resulting lysate was then passed through a 13 mm, 0.2 μm syringe filter (PVDF, Millipore) and 400 μl processed for nucleic acid purification according to the manufacturer's instructions. Nucleic acids were eluted with 100 μL. The nucleic acid extracts were split into two aliquots and stored at −80°C until used in PCR reactions for metabarcoding analysis.

Five aggregate samples (0.2–0.7 ml) from the sea floor were lysed using PrepGem Tissue Kit (MicroGem, Charlottesville, VA). The total volume of each reaction varied to ensure the aggregate sample was only 50% of the reaction volume. The extractions contained 1X green buffer and 1 μl per 100 μl reaction prepGem enzyme and 200 μg ml^{-1} lysozyme. Samples were incubated at 37 °C for 15 min, 75 °C for 15 min and heat inactivated at 95 °C for 5 min. Extracts were filtered through a 13 mm 0.2 μm filter (Millipore). Filtered extracts were concentrated and rinsed with 1 ml TE buffer on a Centricon YM-30 (Amicon, Darmstadt, Germany) to a final volume of approximately 50 μl.

2.5. Small subunit ribosomal RNA (rRNA) metabarcoding library preparation

Recovered nucleic acids from sinking POM, sea floor aggregates and fractionated water column samples were used in PCR reactions to generate amplicon pools for Illumina sequencing of the V9 region of the 18S rRNA and V4 region of the 16S rRNA. Each trap replicate was treated as a unique sample. To avoid inhibition, nucleic acids recovered from sinking POM collected from sediment traps were diluted by 0.01 and sea floor aggregates by 0.1 using PCR grade water (MilliporeSigma). Fractionated water column samples were undiluted. PCR amplifications were performed in triplicate reactions for the water column samples, in 6 replicate reactions for sediment trap samples, and in 9 replicate reactions for the sea floor aggregates.

For 18S rRNA, metabarcoding library preparation followed guidelines of the Earth Microbiome Project without the mammal blocking primer (Thompson et al., 2017). Each 25 μl replicate PCR reactions contained 0.2 μM of each primer, Illumina_Euk1391f forward primer (AATGATACGGCGACCACCGAGATCTACAC TATCGCCGTT CG GTACACACCGCCCGTC) and Illumina EukBr reverse primer with Golay barcode (CAAGCAGAAGACGGCATACGAGAT XXXXXXXXXXXX AGTCAGTCAG CA TGATCCTTCTGCAGGTTCACCTAC), 1x Platinum Hot Start PCR Master Mix (Thermo Fisher Scientific, Waltham, MA, USA), 2 μl DNA template, and PCR-grade water. Thermocycling conditions were as follows, initial denaturation at 94 °C for 2 min, followed by 30 or 35 cycles of 94 °C for 45 s, 57 °C for 60 s, 72 °C for 90 s, and a final extension at 72 °C for 10 min. Thirty cycles were used for sea floor aggregates and water column samples and 35 cycles for sinking POM.

For 16S rRNA, we added additional degeneracies (5′-GGACTACNNGGGTDTCTAAT-3′) to the 806R primer from Apprill et al. (2015). Each 25 μl replicate PCR reaction contained 0.2 μM Illumina 16S 515F forward primer with Golay barcode (AATGATACGGCGACCACCGAGATCTACACGCT XXXXXXXXXXXX TATGGTAATT GT GTGYCAGCMGCCGCGGTAA; Parada et al., 2016), 0.5 μM Illumina 16S 806R primer (CAAGCAGAAGACGGCATACGAGAT AGTCAGCCAG CC GGACTACNNGGGTDTCTAAT; this study), 1x Platinum PCR SuperMix Hi Fidelity (Thermo Fisher Scientific), 1 μl template, and PCR-grade water. Thermocycling conditions were as specified by the Earth Microbiome project: initial denaturation at 94 °C for 2 min, followed by 30 or 35 cycles of 94 °C for 45 s, 50 °C for 60 s, 68 °C for 90 s, and a final extension at 68 °C for 10 min. Thirty cycles were used for sea floor aggregates and water column samples, and 35 cycles for sinking POM.

Replicate sample amplicons were pooled, and purified with AMPure beads according to the manufacturer's protocol (Beckman Coulter, Brea, CA, USA). The resulting purified pool was visualized on a 2.5% agarose gel and quantified using Quant-iT™ dsDNA Assay Kit (Thermo Fisher Scientific) according to the manufacturer's protocol. Pools for each sequencing run contained an equal molar concentration of barcoded amplicons from 96 samples. Multiple sequencing runs for each small subunit rRNA gene were required to sequence all samples. Paired-end sequencing, 2 × 150 bp for 18S and 2 × 250 bp for 16S, was performed at MSU Sequencing Facility (East Lansing, MI) on an Illumina MiSeq platform.

2.6. Processing and analysis of sequencing data

Amplicon libraries were analyzed using the software pipeline Qiime 2.0 (version 2019.1, Bolyen et al., 2019; see Supplementary methods for additional information). De-multiplexed paired end reads were denoised, pair-ends joined, and chimeras removed using DADA2 (Callahan et al., 2016) within Qiime 2.0. Prior to joining paired ends, 18S rRNA sequences were trimmed to 150 nucleotides (nt) by removal of 14 nt and 8 nt from the forward and reverse reads respectively. Similarly, 16S rRNA sequences were trimmed to 250 nt for forward reads (13 nt removed) and 232 nt for reverse reads (22 nt removed) prior to joining. Joined sequences were clustered into amplicon sequence variants (ASVs, 100% similarity). ASVs identified in samples across multiple sequencing runs were merged. For 18S rRNA analysis, ASVs with less than 25 sequences were removed (144,640 sequences removed, 1.5% loss). For 16S rRNA analysis, ASVs with less than 50 sequences were removed (209,985 sequences, 2.4% loss). The removal of rare ASVs was performed to maximize detection of the most abundant ASVs before rarefying the data and to avoid biasing comparisons of ASVs among samples (see below) towards very rare sequences (ASVs containing <0.0003% of total sequences). Taxonomy was assigned to each ASV (Bokulich et al., 2018) using the SILVA_132_rep_set_all_99 database (Quast et al., 2012) for the 16S rRNA sequences and the PR2 database

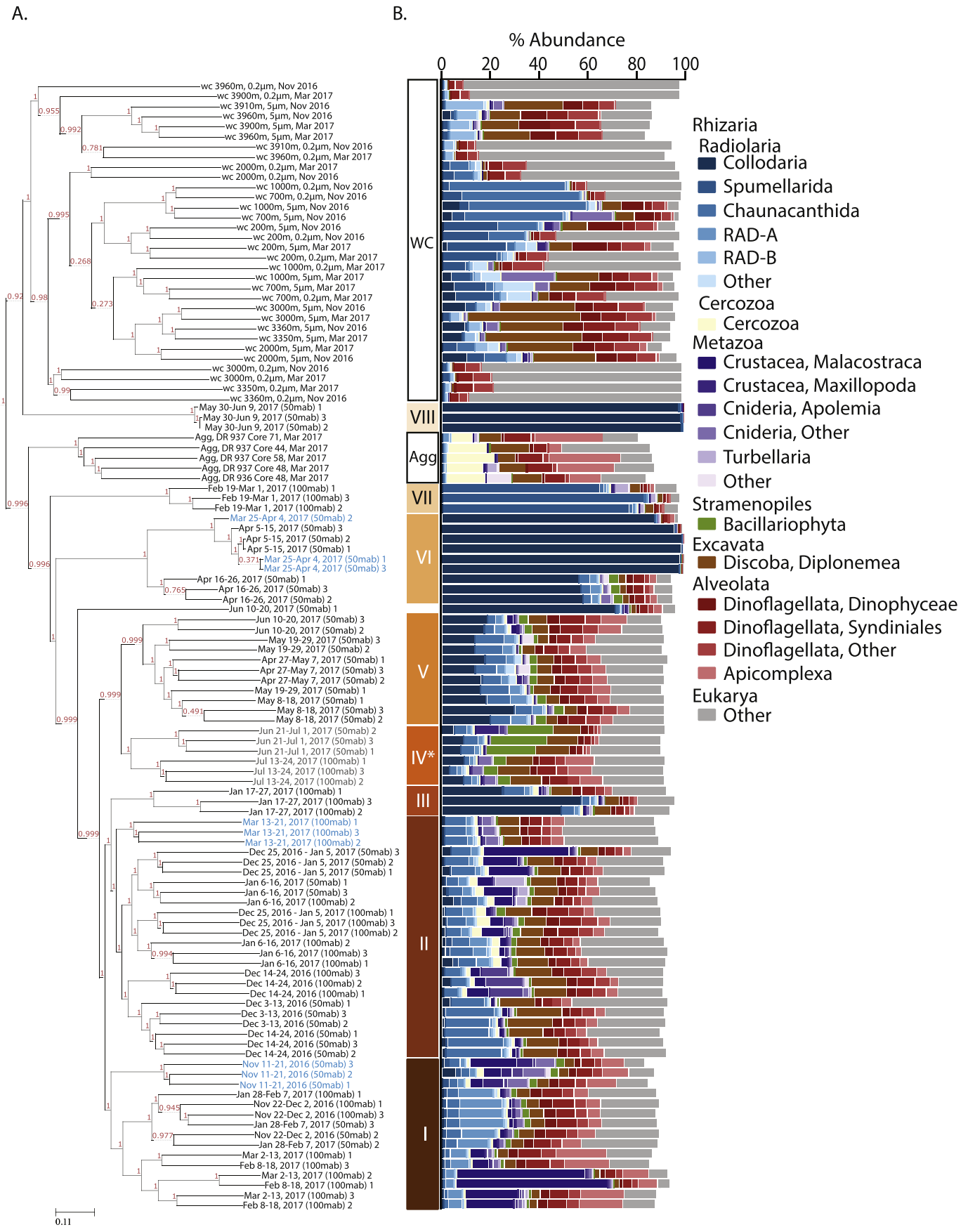

(caption on next page)

Fig. 1. Beta diversity (A) and abundant ASVs (B) of Eukarya from water column (wc), aggregate (Agg) and sediment trap samples. Samples were grouped using cluster analysis by neighbor joining with Bray-Curtis distance and spearman correlation. Values on the tree branches represent the proportion of 1000 bootstrap replications (≥0.5) that supported the nodes (A). The bar graph (B) only includes taxa that account for ≥10% of the sequences within a single sample. ASVs with less than 25 sequences were eliminated and analysis was performed on rarified data (49,000 sequences per sample). In blue are then names of the sinking POM samples collected nearest the date of the water column (wc) samples and in grey are the samples collected at the onset of the high flux event. Water column sample names (wc, open black box) include the depth, size fraction, and sample date. Sea-floor aggregate sample names (Agg, open black box) include the ROV dive number, push core number, and sample date. The sediment traps samples (orange shaded boxes) include the time span of the collection, depth in meters above bottom (mab), and the replicate number. Roman numeral numbered, orange-shaded boxes indicate sediment trap clusters of samples with bootstrap values ≥ 0.9 and Bray-Curtis dissimilarity values < 0.82. Samples collected during the high flux event are indicated (* and sample names in grey).

(version 4.11.1, Guillou et al., 2012) for 18S rRNA sequences. Prior to assigning taxonomy, each database was trained using the respective rRNA sequencing primers.

Filtered sequence data were rarified to 49,000 18S rRNA sequences per sample and 27,500 16S rRNA sequences per sample for subsequent analysis. The q2-diversity plugin was used for PERMANOVA and cluster analysis (Anderson, 2001; Faith et al., 1987; Katoh and Standley, 2013; Mantel, 1967; McDonald et al., 2012; McKinney, 2010; Pearson, 1895; Price et al., 2010; Spearman, 1904; Weiss et al., 2017). Cluster analysis by neighbor joining (1000 bootstraps) with Bray-Curtis distance and Spearman correlation was used to identify samples containing similar rRNA gene communities. Taxa at greater than 10% within a single sample were then identified using taxa bar plots created in Qiime2. If a taxonomic group was present at >10% in a lower taxa level (e.g. L1), it was further investigated at higher taxa levels (L2 to L7). An abundant group was identified at the level where its abundance in higher taxonomic no longer exceeded 10%.

Because the sediment trap samples provided a nearly continuous record of sinking POM in eleven-day intervals, we also investigated the number of ASVs shared between all and successive sediment trap samples using contingency-based filtering within Qiime 2.0 using the filtered, but non-rarified sequence data. These data were used to determine the timing of major transitions in the rRNA gene community.

To identify organisms that may have originally produced the POC collected in sediment traps, we further classified the 16S rRNA sequences categorized as oxyphotobacteria (i.e. chloroplasts or cyanobacteria). Representative sequences of ASVs assigned to Oxyphotobacteria from unfiltered, non-rarified data were compared to the Silva 132 Ref 99 dataset using blastn (Boratyn et al., 2013) and the top 20 hits were used to determine the best taxonomic affiliation of each. ASVs were then classified as cyanobacteria, diatom, coccolithophore, chlorophyte, chrysophyte, euglenoid, dinoflagellate, or land plant. The relative percentage of each within the sediment trap samples was compared.

To determine the diversity of diatoms contributing to the POM within sediment traps during average and high flux periods, 18S rRNA sequences classified as Bacillariophyta from unfiltered, non-rarified data were further compared to the PR2 database (Guillou et al., 2012) using blastn (Boratyn et al., 2013) and the top hit was used to assign sequences to genera. The percent abundance of the diatom genera was compared across all sediment trap samples.

3. Results

Amplicon sequencing of 18S and 16S rRNA genes was utilized to investigate the organismal diversity within POM obtained in fractionated water column samples from two depth profiles (200 m to the sea floor), in sea floor aggregates, and in sinking POM collected in sediment traps over 9 months. From the 112 samples, 9.7 million 18S rRNA sequences and 8.4 million 16S rRNA sequences passed quality control and filtering. Across all sample types, the sequences passing quality control resulted in 10,922 and 4909 unique ASVs (100% similarity), in the 18S and 16S rRNA meta-barcoded libraries, respectively. Filtering rare sequences from the 18S rRNA data (ASVs containing less than < 25 sequences) removed 0.55–2.33% of the sequences from the water column samples, 0.02–3.58% of the sequences from the sinking POM, and 2.34–7.58% of the sequences from the sea floor aggregates. Filtering rare sequences from the 16S rRNA data (ASVs containing less than < 50 sequences) removed 0.62–5.9% of the sequences from the water column samples, 0.76–4.47% of the sequences from the sinking POM, and 3.16–23.12% of the sequences from the sea floor aggregates. The sequence data were analyzed in several ways. Using the filtered and rarefied sequence data, we compared and clustered the samples, then looked for how the major taxa (ASVs representing >10% relative abundance in any one sample) were distributed within those clusters across different sample types and over time in the sinking POM. Using non-rarefied data, we looked for common ASVs across different sample types and between successive sediment trap samples to identify taxa (abundant and rare) consistently present. Lastly, unfiltered, non-rarefied sequence data were used to investigate the source of POC at abyssal depths.

3.1. Comparison of particulate organic matter (POM) collected in different sample types

Taxa within the eukaryotic communities of each sample type (fractionated water column samples, sea floor aggregates, and sediment trap samples) contained similar eukaryotic supergroups at different relative abundances. Eukarya spanned different trophic levels and life strategies including autotrophs, heterotrophic protists, parasitic protists, zooplankton, gelatinous filter feeders and flatworms (Fig. 1). The majority of the sequences were affiliated with Radiolaria, Dinoflagellata, Metazoa, and Discoba. Radiolaria represented 35% of the total 18S rRNA sequences collected in sediment traps over the 9-month period, 27.3% and 18.1% of the >5 μm and <5 μm–0.2 μm fractions from the two water column profiles, respectively, and 2.3% in the sea floor aggregates. Dinoflagellata also accounted for a large proportion of the sequences, 12.2% in sediment traps, 26.8% in the >5 μm and 11.6% in the <5 μm–0.2 μm water column samples, and 12% in the aggregates. Metazoa from 17 phyla were also observed accounting for between 4 and 11% of the total 18S rRNA sequences from each sample type (Fig. S2). The metazoan taxa accounting for more than 10% of the sequences within a single sample were crustacea (amphipods and copepods), cnidaria, and platyhelminthes (Fig. 1). The fractionated water column samples and sea floor aggregates had greater relative abundance of Discoba (11.1% and 21.3%, respectively). All three sample types contained a large percentage (19%–38%) of unassigned 18S rRNA sequences.

The 16S rRNA community from all sample types included photoautotrophs, chloroplasts of eukaryotic algae, known colonizers of particulates, those associated within or on eukaryotic hosts, chemoautotrophs, and free-living bacterioplankton (Fig. 2). The taxa comprising the 16S rRNA community in the water column were distinct from the communities in the sinking POM collected in sediment traps and in sea floor aggregates. Water column samples regardless of the size fraction had higher relative abundances of taxa normally associated with free-living bacterioplankton, including Thaumarchaeota (14.9%), SAR11 (8.7%), Thiomicrospirales (SUP05 8.0%), SAR 406 (6.1%), and SAR 324 (5.4%). Taxa associated with the origin of the POM or with a particle-attached lifestyle, were at higher relative abundances in the sediment trap and sea floor aggregate samples compared to the water column. Larger relative proportions of Bacteroidia (12%–33%) and

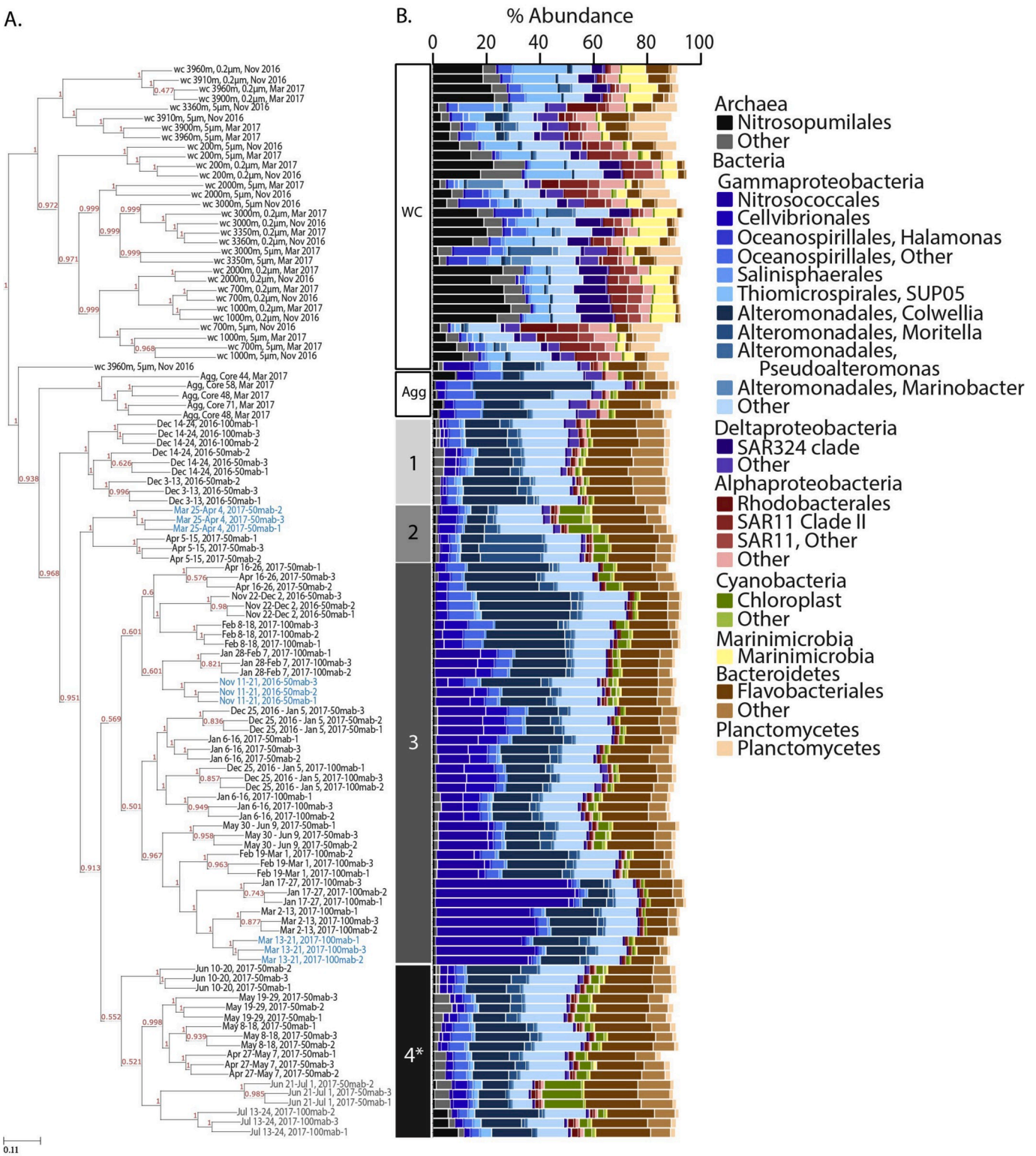

Fig. 2. Beta diversity (A) and abundant ASVs (B) of Bacteria and Archaea from water column (wc), aggregate (Agg), and sediment trap samples. Cluster analysis was performed by neighbor joining with Bray-Curtis distance and spearman correlation (A). Values on the tree branches represent the proportion (>0.5) of 1000 bootstrap replications that supported the nodes. The bar graph (B) only includes taxa that account for ≥10% of the sequences within a single sample. ASVs with less than 50 sequences were eliminated and analysis was performed on rarified data (27,500 sequences per sample). Sample types and names are as defined in Fig. 1. Numbered, greyscale boxes indicate clusters of samples with bootstrap values ≥ 0.9. Samples collected during the high flux event are indicated (* and sample names in grey).

Table 1
Bray Curtis dissimilarity within and between different sample types using rarified 18S rRNA gene sequences (49,000 seqeuences per sample).

	Trap	Water Column >5um	Water Column <5-0.2μm	Seafloor Aggregate
Trap (9 months, n=75, 25 samples x 3 replicates)	0.791 (0.011-0.998)	0.908 (0.705-0.999)	0.960 (0.752-1.0)	0.930 (0.828-0.999)
Water Column >5um (n=16), 200m-3960m	9.34 (0.001)	0.764 (0.372-0.913)	0.904 (0.422-0.988)	0.965 (0.916-0.990)
Water Column <5-0.2μm (n=16), 200m-3960m	7.50 (0.001)	2.93 (0.001)	0.933 (0.457-0.990)	0.990 (0.981-0.997)
Seafloor Aggregate (n=5)	5.66 (0.001)	6.63 (0.002)	3.99 (0.001)	0.639 (0.575-0.698)

Shaded grey boxes = Bray Curtis dissimilarity average (mininium-maximum); Between trap samples (n=25, replicates collapsed): 18S= 0.781(0.050-0.997)
Unshaded boxes = Pairwise permanova pseudo-F (p-value), 999 permutations

gammaproteobacteria from Alteromonadales (10%–47%), Nitrosococcales (0.1%–52%), and Cellvibrionales (3%–18%) were found in sediment trap samples and the sea floor aggregates.

Sample relatedness based on the compositional dissimilarity (Bray-Curtis metric and using rarified sequence data) indicated that the sample types, sediment trap, Niskin, and sea floor aggregates captured different POM communities. The average Bray-Curtis dissimilarity between the sample types using the 18S rRNA gene sequences was >0.9 (Table 1), and using the 16S rRNA, >0.7 (Table 2). PERMANOVA for both the 18S and 16S rRNA data sets, indicated there was a significant difference between the communities collected in the different sample types (Tables 1 and 2). Cluster analysis of either rRNA gene using Bray-Curtis distance with Spearman correlation (Figs. 1 and 2) confirmed these results. In general, each sample type grouped together with two exceptions. The >5 μm fraction at 3960 m from November 2016 peripherally grouped with the sinking POM and sea floor aggregate samples based on the 16S rRNA sequences, and the sediment trap sample from May 30 to June 9 peripherally grouped with the fractionated water column samples based on the 18S rRNA sequences.

For the POM collected in sediment traps, the 18S rRNA community was more variable within subsamples and between trap samples than the 16S rRNA community. Subsamples (n = 3) from 19 of 25 samples clustered together based on the 18S rRNA data (Fig. 1, Bray-Curtis dissimilarity of replicate samples 0.017 to 0.655), whereas the replicate samples clustered together based on the 16S rRNA data (Fig. 2, Bray-Curtis dissimilarity of replicate samples 0.106–0.310). In addition, the Bray-Curtis dissimilarity observed among 18S rRNA sequence communities was 0.05–0.997, indicating that some samples were nearly identical while others harbored completely different communities. The Bray-Curtis dissimilarity range was 0.253–0.816 among 16S rRNA sequence communities, indicating more shared bacterial and archaeal ASVs compared to the eukaryotic ASVs among samples.

3.2. Common amplicon sequence variants (ASVs) in sinking POM

We identified a core sinking POM community within the sediment trap samples collected at 3900 m and 3950 m over nine months. Two eukaryal and 39 bacterial ASVs were found in every sediment trap sample collected (Table 3). The proportion of these taxa varied over time. The two eukaryal ASVs, radiolarians affiliated with RAD-A and *Chaunacanthida*, accounted for between 0.06% and 23% of the eukaryotic sequences in each sample (Figs. 1 and 3A). The core 16S rRNA community accounted for 23%–52% (average 40%) of the sequences in each sample and spanned many different bacterial phyla. The majority were known colonizers of particulates (e.g. *Alteromonadales, Flavobacteriales, Rhodobacterales*, and *Oceanospirillales*) and typically found at depth (Figs. 2 and 3B). Less abundant but still components of the core community were taxa associated with guts and surfaces of eukaryotes (e.g. *Vibrio*), the origin of POM (chloroplasts and cyanobacteria), and chemoautotrophs (e.g. SUP05).

A low proportion of the core sediment trap POM community was present within the water column samples. In general, as the water column sample depth increased, the number of ASV types belonging to the core sediment trap bacterial community also increased. The relative percentage of total sequences in the water column samples that were members of the core sinking bacterial community averaged 10% (range 3%–30%). The highest relative percentage was from the only water column sample containing all 39 ASVs: the >5 μm fraction from 3960 m collected in November 2016. Of the two eukaryal ASVs present in all the sediment trap samples, only one affiliated with Chaunacanthida was present at all depths in the two water column profiles.

In addition, the deep-water column samples (>3000 m) and sediment trap samples had very few shared ASVs. The November 10–11, 2016 water column samples in the >5 μm size fraction and deeper than 3000 m depth shared 49 eukaryal ASVs with the sinking POM collected from November 11–21, 2016. These 49 ASVs were only 1.9% of the total ASVs from water column samples in the >5 μm size fraction at ≥ 3000 m (2577 total ASVs) and 3.2% of the total sinking POM ASVs (1496 total ASVs). The relative percentage of sequences belonging to those ASVs in the deep-water column samples and sediment trap was 19% and 17%, respectively. The March 23–25, 2017 samples of the >5 μm size fraction and deeper than 3000 m had fewer eukaryal ASVs in common with sinking POM and those ASVs were at lower relative abundances. The water column sample had 26 and 8 eukaryal ASVs in common with the March 13–22, 2017 and March 25-April 4, 2017 sediment trap samples, respectively. These ASVs were ≤1% of the total ASVs from the >5 μm fraction below 3000 m (2494 total ASVs) and represented 13% (26 ASVs) and 3% (8 ASVs) of total sequences in those samples. The shared ASVs were 1.5% and 2.7% of the total ASVs in the sinking POM traps collected before and after the water column samples, respectively. The trap sample before the water samples had a higher relative percentage (16%) of those sequences than the trap sample after (0.8%).

The large light green sea floor aggregates collected in mid-March (Supp. Fig. 1) offered an opportunity to observe the community diversity of a specific category of POM. The dominant taxa within these aggregates included Apicomplexa (20% average relative abundance), Cercozoa (15%), parasitic dinoflagellates belonging to Syndiniales (9%), and Discoba (11%). Ochrophyta accounted for an average of 5% of 18S rRNA gene sequences. Pelagophyceae (1.7%) and Dinophyceae (1.2%) dominated over diatoms and golden algae (<0.5%). Accounting for the majority of 16S rRNA sequences were Gammaproteobacteria (average relative abundance 64%) belonging to Colwellia (22%), Cellvibrionales (11%) and Oceanosprilles (10%). Other groups included Bacteroidetes (15.8%), Thaumarchaeota (6%), Planctomycetes (3%), and chloroplast (1.3%) sequences belonging to green algae, pelagophyceae, and diatoms. Highly variable were the rRNA communities between these five sea-floor aggregate samples. They contained a total of 1572 eukaryal ASVs with an average of 690 ASVs per aggregate. Of those, 155 ASVs were found in all aggregates and accounted for nearly half of the sequences (46–49%). The 16S rRNA gene sequences within the aggregates

Table 2
Bray Curtis dissimilarity within and between different sample types using rarified 16S rRNA gene sequences (27,500 seqeuences per sample).

	Trap	Water Column >5um	Water Column <5-0.2μm	Seafloor Aggregate
Trap (9 months, n=75, 25 samples x 3 replicates)	0.534 (0.096-0.832)	0.889 (0.486-0.976)	0.949 (0.845-0.991)	0.776 (0.635-0.866)
Water Column >5um (n=16), 200m-3960m	32.77 (0.001)	0.694(0.232-0.93)	0.740 (0.281-0.969)	0.945 (0.814-0.986)
Water Column <5-0.2μm (n=16), 200m-3960m	45.92 (0.001)	4.50 (0.001)	0.610 (0.143-0.937)	0.985 (0.938-0.998)
Seafloor Aggregate (n=5)	12.02 (0.001)	9.87 (0.001)	13.85 (0.001)	0.442 (0.303-0.628)

Shaded grey boxes = Bray Curtis dissimilarity average (mininium-maximum); Between trap samples (n=25, replicates collapsed): 16S= 0.525 (0.253-0.816)
Unshaded boxes = Pairwise permanova pseudo-F (p-value), 999 permutations

encoded 1200 total ASVs with an average of 608 ASVs per sample. Common among all aggregate samples were 205 16S rRNA ASVs accounting for between 57 and 72% of the sequences in each aggregate sample. These common aggregate ASVs accounted for less than half (for 18S rRNA 17–37% and for 16S rRNA 26–42%) of the ASVs in the sediment trap samples (November 11 to March 3) preceding the collection date of the sea floor aggregates.

3.3. Time series of POC and sinking POM

Changes in the magnitude of particle flux over time collected in sediment traps at 50 mab from November 2016 to July 2017 (Fig. 3) were similar to concurrent observations from a 600 mab trap at Station M and captured two different POC flux periods (Smith et al., 2018). From November 2016 to mid-June 2017, POC flux was average, 6.9 ± 2.1 mg C • m^{-2} • d^{-1}, which is within the 29-year average ± σ at Station M for the 50 mab sediment trap (8.3 ± 7.9 mg C • m^{-2} • d^{-1}). From June 21 to July 24, the POC flux exceeded the long-term mean + 2 σ, indicative of an episodic pulse event. The high flux event from June 21-July 25 accounted for 44% of the POC collected during this study. Coinciding with the high-flux period shown here, a pulse event at 600 mab followed a period of high net primary productivity and modeled changes in export flux out of the surface by 10 days (Smith et al., 2018).

The assemblage of eukaryotic organisms within the particles changed more frequently over the nine-month period than the assemblage of organisms detected by their 16S rRNA genes, as defined by the cluster assignments based on community composition (Figs. 1–3). Eleven transitions were observed among the eight distinct 18S rRNA communities over time (Fig. 3). These communities differed primarily by their relative abundance of metazoans, radiolarians, and diatoms (Bacillariophyta, Figs. 1 and 3). Seven transitions were observed among the four distinct 16S rRNA communities (Fig. 3). These communities differed primarily by their relative abundance and presence of various Gammaproteobacteria, *Bacteriodia,* cyanobacteria, archaea, and Alphaproteobacteria (Figs. 2 and 3, see below). Below, we assess how transitions from one particle-associated community to another related to the magnitude of POC flux from winter to early summer.

3.3.1. Sinking POM during winter to early spring

The months from November 2016 to late March 2017 were characterized by average POC flux with no or very little accumulation of POM on the sea floor (Fig. 3). The eukaryal community during this period transitioned seven times and the 16S rRNA community transitioned three times. During most of this period, the eukaryal community alternated between 18S-I or 18S-II clusters (Figs. 1 and 3C). Samples within these clusters contained most total detected metazoan rRNA sequences (Fig. 1, Fig. 3A and Suppl. Fig. 2), including amphipods, copepods, cnidaria, ctenophores, anthozoa, gastropods, larvaceans, annelids, and flatworms. Clusters 18S-I and 18S-II also contained the greatest proportion of the radiolarian orders RAD-A and *Chaunacanthida*, respectively. The dominance of these two community assemblages was interrupted twice (January 17–27 and February 19-March 1) by assemblages composed primarily of radiolarians that were present for a much shorter duration (11 days each, Fig. 3). Neither of these interruptions in the 18S rRNA assemblage corresponded to a change in the 16S rRNA sample cluster (Fig. 3). The eukaryal communities were dominated by different Polycystinea radiolarians, first by Collodaria (24–57% of 18S rRNA sequences, cluster 18S-III) and then *Spumellaria* (>65% of 18S rRNA sequences, cluster 18S-VII).

The 16S rRNA cluster 16S-3 (Figs. 2 and 3) was present for the 110 of 131 days of the winter to early spring period. Samples within this cluster contained the highest relative abundances of *Gammaproteobacteria* (>55% of the sequences), specifically, *Nitrococcales* and *Colwellia*. Only once and for 22 days was cluster 16S-1 present and its appearance coincided with a change to the 18S-II community on December 3, 2016. The bacterial community of these samples contained lower relative percentages of *Nitrosococcales* and *Cellvibrionales* and higher relative percentages of group II archaea, OM183, and Bacteroidetes (Fig. 3B). During this short period when 16S-I cluster was present, detrital aggregates appeared on the sea floor and remained present for a brief time after the transition back to 16S rRNA cluster 16S-3. No change in POC flux was observed.

Despite many transitions between the various community assemblages during the winter period, 35 18S rRNA ASVs and 51 16S rRNA ASVs were present in every single 11-day sample from November 11 to March 22. Consistently present were 18S rRNA ASVs affiliated with Rhizaria (*Chaunacanthida*, RAD-A, and *Cercozoa*), *Diplonemea*, *Dinoflagellata* (*Syndiniales* and *Dinophyceae*), *Metazoa* (*Nanomia* and *Ctenophora*), and *Stramenopiles* (*Bacillariophyta*, *Chrysophyceae*, and *Oomycota*). In addition to the core 16S rRNA community (31–52% of the sequences, Table 2), ASVs consistently present included marine group II euryarchaea, Gracilibacteria, *Polaribacter*, and *Marinicella,* and *Profundimonas*.

3.3.2. Sinking POM leading up to the high-flux event

In March, when POC flux was still within the time-series average, a community dominated by *Collodaria* radiolarian sequences (Cluster 18S-VI) persisted for 33 days, initially at relative abundances over 99% and decreasing to 65.5% by mid-April (Fig. 1). The transition to this radiolarian-dominant community was rapid. Only a 4-day gap in sediment trap sampling coinciding with its servicing, occurred between the March 13–21 (18S-II) and March 25-April 4 (18S-VI) samples. The dominant ASV affiliated with *Collodaria* was not detected in the previous trap sample nor was it detected at any depth in the March 2017 water column samples. During the period when *Collodaria* dominated, the 16S rRNA community transitioned twice. The16S rRNA cluster 16S-2 was present for the first 22 days and contained different relative abundances of *Moritella* and *Colwellia* compared to previous timepoints and the highest relative abundances of green algal 16S rRNA chloroplast sequences observed over nine months (Figs. 2 and 4). The 16S rRNA community then returned to cluster 16-3 (Fig. 3) when the eukaryal community became relatively more diverse (Figs. 1 and 3).

When POM began to accumulate on the sea floor in late April, a new 16S rRNA community (cluster 16S-4) was observed that dominated the remaining days of the deployment (Fig. 3). The 16S rRNA community (cluster 16S-4) contained higher relative abundances of *Bacteroidetes*,

Table 3
Taxa identity and proportion of ASVs found in all sediment trap samples.

Library[a]	Phylogenetic Affiliation of Amplified Sequence Variants (ASVs)	Number of ASVs in all sediment trap samples	Number of sequences represented by ASVs in all sediment trap samples	Proportion of reads of ASVs in all (average and range) per sample's total reads			Proportion of in all ASVs per total reads of ASV's phylogenetic affiliation per sample	
				average	max	min	max	min
18S rRNA	Total Eukaryal ASVs found in All Sediment Trap Samples	2	4,99,539	0.0782	0.2301	0.0006	na	na
18S rRNA	Eukaryota; Rhizaria; Radiolaria; RAD-A; RAD-A	1	1,50,118	0.0231	0.1173	0.0001	1	0.220
18S rRNA	Eukaryota; Rhizaria; Radiolaria; Acantharea; Chaunacanthida	1	3,49,421	0.0550	0.2195	0.0004	1	0.966
16S rRNA	Total Bacterial ASVs found in All Sediment Trap Samples	39	22,92,050	0.4011	0.5221	0.2303	na	na
16S rRNA	Bacteria; Proteobacteria; Gammaproteobacteria; Alteromonadales; Colwelliaceae; Colwellia	6	6,15,925	0.1067	0.2584	0.0409	0.898	0.408
16S rRNA	Bacteria; Proteobacteria; Gammaproteobacteria; Nitrosococcales; Methylophagaceae; Marine Methylotrophic Group 3	1	2,08,724	0.0424	0.2957	0.0001	1	0.096
16S rRNA	Bacteria; Proteobacteria; Gammaproteobacteria; Alteromonadales; Moritellaceae; Moritella	1	2,17,330	0.0368	0.2361	0.0031	1	0.989
16S rRNA	Bacteria; Bacteroidetes; Bacteroidia; Sphingobacteriales; KD1-131; uncultured organism	1	1,16,551	0.0209	0.0642	0.0020	1	0.969
16S rRNA	Bacteria; Proteobacteria; Gammaproteobacteria; Alteromonadales; Shewanellaceae; Psychrobium	1	1,18,601	0.0207	0.0453	0.0013	1	0.860
16S rRNA	Bacteria; Proteobacteria; Gammaproteobacteria; Alteromonadales; Psychromonadaceae; Psychromonas	1	1,18,434	0.0197	0.0509	0.0068	1	0.774
16S rRNA	Bacteria; Epsilonbacteraeota; Campylobacteria; Campylobacterales; Arcobacteraceae; Arcobacter	2	1,02,012	0.0190	0.0761	0.0035	0.963	0.552
16S rRNA	Bacteria; Proteobacteria; Gammaproteobacteria; Cellvibrionales; Spongiibacteraceae; BD1-7 clade	2	1,08,523	0.0187	0.0628	0.0019	0.681	0.184
16S rRNA	Bacteria; Proteobacteria; Gammaproteobacteria; Thiomicrospirales; Thioglobaceae; SUP05 cluster	2	78,813	0.0134	0.0411	0.0021	1	0.860
16S rRNA	Bacteria; Cyanobacteria; Oxyphotobacteria; Chloroplast; Prasinoderma coloniale; Prasinoderma coloniale	1	75,761	0.0121	0.0818	0.0006	1	0.974
16S rRNA	Bacteria; Bacteroidetes; Bacteroidia; Flavobacteriales; Flavobacteriaceae; Flavicella	1	65,206	0.0105	0.0454	0.0005	1	0.203
16S rRNA	Bacteria; Proteobacteria; Gammaproteobacteria; Cellvibrionales; Cellvibrionaceae; Umboniibacter	1	50,380	0.0089	0.0281	0.0005	1	0.981
16S rRNA	Bacteria; Bacteroidetes; Bacteroidia; Flavobacteriales; Flavobacteriaceae; Psychroserpens	1	41,687	0.0072	0.0299	0.0007	1	0.191
16S rRNA	Bacteria; Bacteroidetes; Bacteroidia; Flavobacteriales; Flavobacteriaceae	1	39,573	0.0066	0.0164	0.0004	0.703	0.077
16S rRNA	Bacteria; Proteobacteria; Gammaproteobacteria; Vibrionales; Vibrionaceae; Vibrio	1	34,114	0.0058	0.0318	0.0005	1	0.141
16S rRNA	Bacteria; Cyanobacteria; Oxyphotobacteria; Synechococcales; Cyanobiaceae; Synechococcus CC9902	1	34,516	0.0057	0.0184	0.0013	1	0.610
16S rRNA	Bacteria; Proteobacteria; Gammaproteobacteria; Alteromonadales; Pseudoalteromonadaceae; Pseudoalteromonas	1	30,586	0.0055	0.0136	0.0017	1	0.625
16S rRNA	Bacteria; Proteobacteria; Gammaproteobacteria; Cellvibrionales; Spongiibacteraceae; Sinobacterium	1	27,727	0.0050	0.0212	0.0007	1	0.316
16S rRNA	Bacteria; Proteobacteria; Gammaproteobacteria; Oceanospirillales; Oleiphilaceae; Oleiphilus	1	27,787	0.0047	0.0116	0.0007	1	0.088
16S rRNA	Bacteria; Proteobacteria; Gammaproteobacteria; OM182 clade; hydrothermal vent metagenome	1	20,611	0.0037	0.0115	0.0005	1	0.993
16S rRNA	Bacteria; Lentisphaerae; Lentisphaeria; Lentisphaerales; Lentisphaeraceae; Lentisphaera	2	17,479	0.0033	0.0147	0.0004	0.729	0.056
16S rRNA	Bacteria; Proteobacteria; Gammaproteobacteria; Oceanospirillales; Saccharospirillaceae; Oleispira	1	19,419	0.0032	0.0094	0.0004	1	0.863
16S rRNA	Bacteria; Proteobacteria; Alphaproteobacteria; Rhodobacterales; Rhodobacteraceae	1	18,072	0.0031	0.0081	0.0011	1	0.241
16S rRNA	Bacteria; Bacteroidetes; Bacteroidia; Flavobacteriales; Flavobacteriaceae; Pseudofulvibacter	1	16,740	0.0029	0.0090	0.0006	1	0.306
16S rRNA	Bacteria; Proteobacteria; Gammaproteobacteria; Gammaproteobacteria; Marinicella	1	17,382	0.0029	0.0081	0.0004	1	0.376
16S rRNA	Bacteria; Bacteroidetes; Bacteroidia; Cytophagales; Cyclobacteriaceae; uncultured	1	15,437	0.0028	0.0079	0.0006	0.408	0.018
16S rRNA	Bacteria; Planctomycetes; Planctomycetacia; Pirellulales; Pirellulaceae; Rhodopirellula	1	15,774	0.0027	0.0059	0.0008	1	0.583
		1	16,775	0.0026	0.0074	0.0002	1	0.584

(*continued on next page*)

Table 3 (*continued*)

Library[a]	Phylogenetic Affiliation of Amplified Sequence Variants (ASVs)	Number of ASVs in all sediment trap samples	Number of sequences represented by ASVs in all sediment trap samples	Proportion of reads of ASVs in all (average and range) per sample's total reads			Proportion of in all ASVs per total reads of ASV's phylogenetic affiliation per sample	
				average	max	min	max	min
16S rRNA	Bacteria; Proteobacteria; Alphaproteobacteria; Sphingomonadales; Sphingomonadaceae; Erythrobacter							
16S rRNA	Bacteria; Proteobacteria; Gammaproteobacteria; UBA10353 marine group; uncultured organism; uncultured organism	1	14,441	0.0025	0.0060	0.0009	1	0.741
16S rRNA	Bacteria; Bacteroidetes; Bacteroidia; Flavobacteriales; Crocinitomicaceae; Salinirepens	1	7,670	0.0013	0.0049	0.0002	0.591	0.054

na = not applicable.

[a] Total 18S rRNA sequences in trap samples = 6,100,209; total 16S rRNA sequences in trap samples = 5,747,599.

archaea, and chloroplasts (Figs. 2–4). The corresponding change in the eukaryal community was present for 44 days from April 27 to June 20 and contained a mixed eukaryal community of radiolaria and alveolates with smaller contributions from various metazoans relative to winter samples (Figs. 1 and 3). For 10 days from May 30-June 9, the POM community transitioned back to a radiolarian dominant community (Cluster 18S-VIII). Radiolaria from the order *Collodaria* represented the majority of the sequences (98%) and were present in the sample previous to and after the May30-June 9 sample. The 16S rRNA community also transitioned to 16S-3 for these 10 days.

Part of the community observed in the April 16–26 sample (Cluster 18S-VI and 16S-3) persisted through the end of June indicating that this sub-community had a lasting influence on the sinking POM. The two samples collected between April 16 and May 7 shared 152 18S rRNA ASVs and 197 16S rRNA ASVs. Those ASVs represented 48% of total 18S rRNA sequences and 75.5% of the total 16S rRNA sequences in the sample collected April 27-May 7 (Cluster 18S-V and 16S-4). Of those, 73 eukaryal ASVs were still present until June 20 (excluding the radiolarian dominated, May 30-June 9 sample), accounting for 21% of the 18S rRNA sequences. The taxa of the eukaryal sub-community were affiliated with *Rhizaria* (*Collodaria*, *Chaunacanthida*, RAD-A, RAD-B, and *Cercozoa*), *Diplonemea*, *Stramenopiles* (*Bacillariophyta* and *Labyrinthulea*), *Dinoflagellata* (*Syndiniales* and *Dinophyceae*), *Chlorophyta*, and *Metazoa* (*Nanomia* and *Ctenophora*). During the same period (April 16-June 20), 112 16S rRNA ASVs were still present accounting for 57% of the sequences. Taxa included the core 16S rRNA community (34–46% of the sequences, Table 2) along with group II euryarchaea, *Thaumarchaeota*, *Actinobacteria*, *Bacteriodia* (*Chitinophagales*, *Cryomorphaceae*, marine groups NS7 and NS9, and *Sphingobacteriales*), *Lentisphaerae*, *Patescibacteria*, *Gammaproteobacteria* (*Arenicellaceae*, *Nitrinocolaceae*, and *Sacchrospirllaceae)*, *Verrucomicrobia*, and green algal chloroplasts from *Prasinoderma*.

3.3.3. Sinking POM during the high-flux event

With the onset of the high flux event (June 21), sea-floor aggregate coverage reached 99% and sea-floor fluorescence was the highest observed during this study (Fig. 3). The particles sinking during this period were composed of phytoplankton, radiolaria, and parasitic protists (cluster 18S-IV) during which time the samples contained highest relative abundance of diatom sequences (Figs, 1 and 4). Only two samples were collected during this high flux event because the sinking POM clogged the trap opening. The samples were separated by 10 days and collected at different trap depths (50 mab then 100 mab). The two high POC flux samples shared 225 16S rRNA ASVs and 155 18S rRNA ASVs. The core 16S rRNA community accounted for a lower relative percentage (23%) of the sequences during the onset of the high flux event. Some of the ASVs common between the two samples included taxa associated with phytoplankton blooms including SAR116, *Roseobacter* NAC11-7, OM27, OM43, OM60 (NOR5), and SAR86. Common 18S rRNA ASVs were affiliated with *Rhizaria* (*Collodaria*, *Spumellarida*, Acantharea, RAD-A, RAD-B, and *Cercozoa*), *Diplonemea*, *Stramenopiles* (*Bacillariophyta, Dictyochophyceace, Pelagophyceae, Oomycota,* MAST-1C, and *Labyrinthulea*), *Dinoflagellata* (*Syndiniales* and *Dinophyceae*), *Chlorophyta*, *Streptophyta*, *Metazoa* (*Apolemia*, *Nanomia* and other *Hydrozoa*). The community of the high flux event was significantly different than those associated with average POC flux during the study period. Pairwise PERMANOVA using Bray-Curtis dissimilarity of the high flux trap samples versus non-high flux samples were significant for 18S (pseudo-F 3.5363, p-value 0.001, 999 permutations) and 16S (all sequences = pseudo-F 7.903, p-value 0.001, 999 permutations and eukarya removed pseudo-F = 7.914, p-value 0.001, 999 permutations) rRNA sequences.

3.4. Genetic identification of primary producers in exported carbon

Over the nine-month period, we observed a seasonal shift in the relative influence of autotrophic phytoplankton within the sinking particles, with low percent contributions to the total sequence reads in the winter months and increasing to more than 15% of the total reads during the high flux event (Figs. 3 and 4a). The most frequently detected autotrophs generating the exported POC at Station M included *Synechococcus*, chlorophytes, and diatoms; each having a different relative contribution over the season. In the early winter, the majority of sequences from photosynthetic organisms were affiliated with either cyanobacteria, primarily *Synechococcus*, or diatoms (Fig. 4b). In January, the relative abundance of chlorophyte sequences began to increase, accounting for up to 75% of the oxyphotobacteria 16S rRNA sequences through March. Almost all chlorophyte chloroplast sequences were most similar to *Prasinoderma*. Beginning mid-April, chloroplast sequences from diatoms increased in relative abundance and were often more dominant than chlorophyte sequences. When the high POC flux event occurred in June, most photoautotropic 16S rRNA sequences were associated with diatom chloroplasts (92%); the majority assigned to the genus *Lauderia* (78% of diatom chloroplast reads), a member of the Thalassiosirales diatom lineage.

The diversity of sequences (18S rRNA) assigned to diatoms (i.e. Bacillariophyta) changed seasonally over the 9-month deployment (Fig. 4c) and with the onset of the high flux event. Winter diatom sequences were primarily composed of *Chaetoceros* (*C. didymus*, *C. neogracile*, *C. socialis*, *C. sp.*) and a raphid pennate. These raphid pennate sequences most likely belong to small *Nitzschia bicapitata*-like cells readily observed by microscopy (CAD, personal observation). A major change in the diatom community occurred in May while POC fluxes were still low but when aggregate cover on the sea floor increased (Fig. 3). *Thalassiosira*, *Minidiscus*, and *Actinocyclus* were the major genera

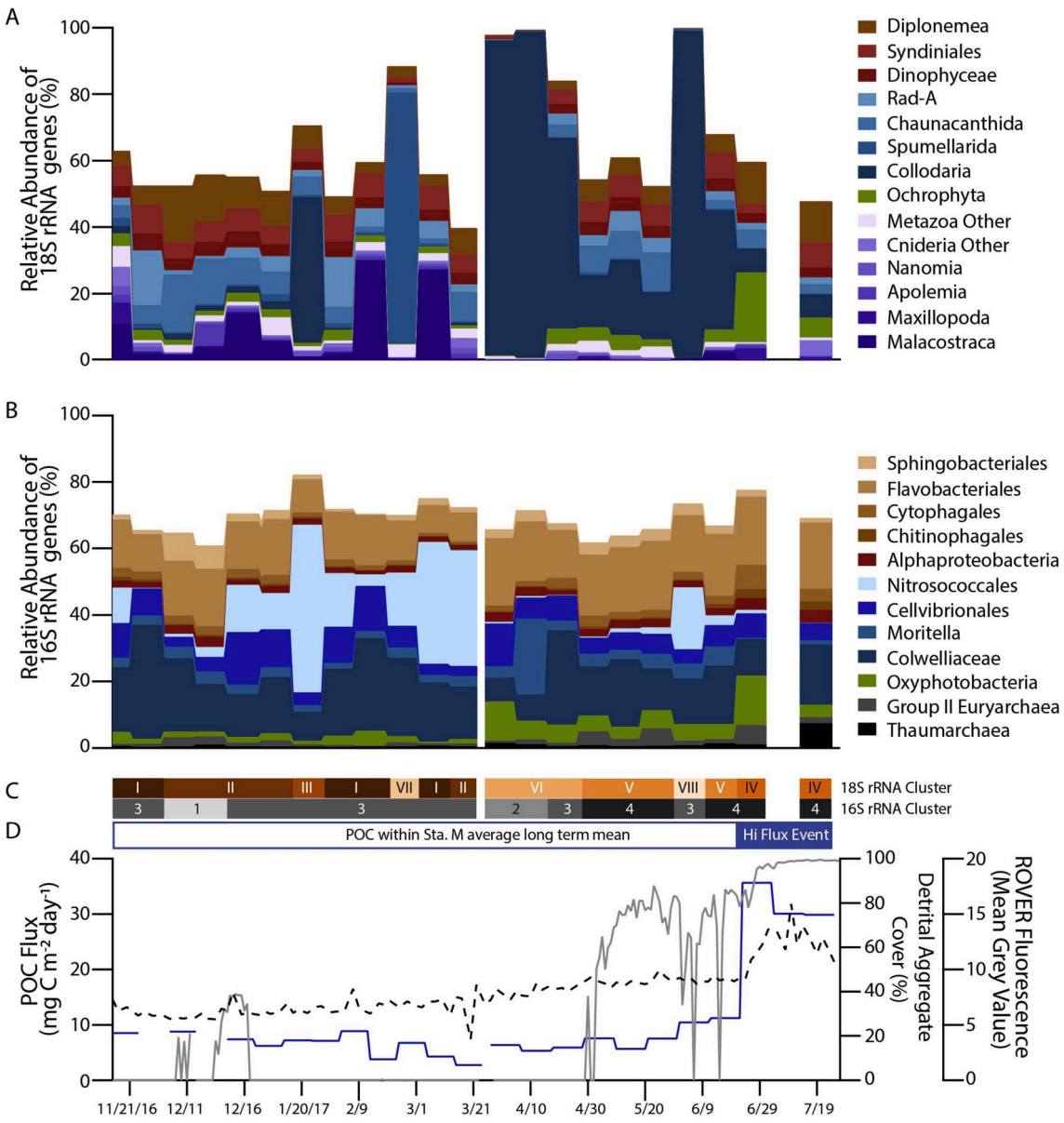

Fig. 3. Nine-month time series of a subset of eukaryal (A), bacterial and archaeal (B) taxa, the 18S and 16S rRNA sample clusters (C) and measurements of particulates at 50mab and the sea floor (D). Orange-scale (18S rRNA) and greyscale (16S rRNA) boxes specify the sample cluster group of the sinking particulates (see Figs. 1 and 2). POC flux (D, blue line, left axis) were made from sinking material collected in traps deployed at 50mab containing formaldehyde. For the majority of the deployment the POC flux was within the 29-year long term average ± σ (C, open blue box) until the onset of a high flux event on June 21 (solid blue box). The chlorophyll fluorescence of particulates on the sea floor (D, black dashed line) and the percentage of the sea floor covered by detrital aggregates (D, grey line) were determined from sea floor images collected from the ROVER.

present during this period, along with the coastally-associated genera *Skeletonema* and *Ditylum*. When the high POC flux event occurred in late June, diatoms contributed a greater percentage of the total 18S rRNA sequence reads (Figs. 1 and 4a). During this period, 64% of the diatom 18S rRNA sequences were assigned to *Thalassiosira aestivalis*, a species not detected in any previous sample.

4. Discussion

Carbon export and sequestration to the deep ocean is influenced both by the photosynthetic organisms that produce POC in the upper ocean and the heterotrophic organisms that intercept and reprocess that POC in the water column as it sinks. Here, we use the genetic signature of organisms (small subunit rRNA gene) retained within POM (1) to compare communities within particulates collected using different sampling methods and (2) to identify ecological processes that influence deep POC export in the California current. Although not discussed in detail here, many major taxonomic groups previously identified as important contributors to POC flux were indeed present in the data over the 9 months (e.g. Haptophytes, Ciliates, Salps, Firmicutes, Vibrio) but sporadically or at lower relative abundances. We focused on discussing those taxa that were either at high relative abundance (>10% relative abundance in a single sample) or were represented by ASVs common within and between successive sediment trap samples.

4.1. Comparison of sample collection methods

Many previous studies have utilized Niskin sampling followed by serial filtration to enrich for the particle attached community (Ganesh et al., 2013; Gutierrez-Rodriguez et al., 2019; Liu et al., 2018; Mestre et al., 2018; Peoples et al., 2018; Xu et al., 2018). However, studies that sample sinking particles in traps typically find that POM responsible for

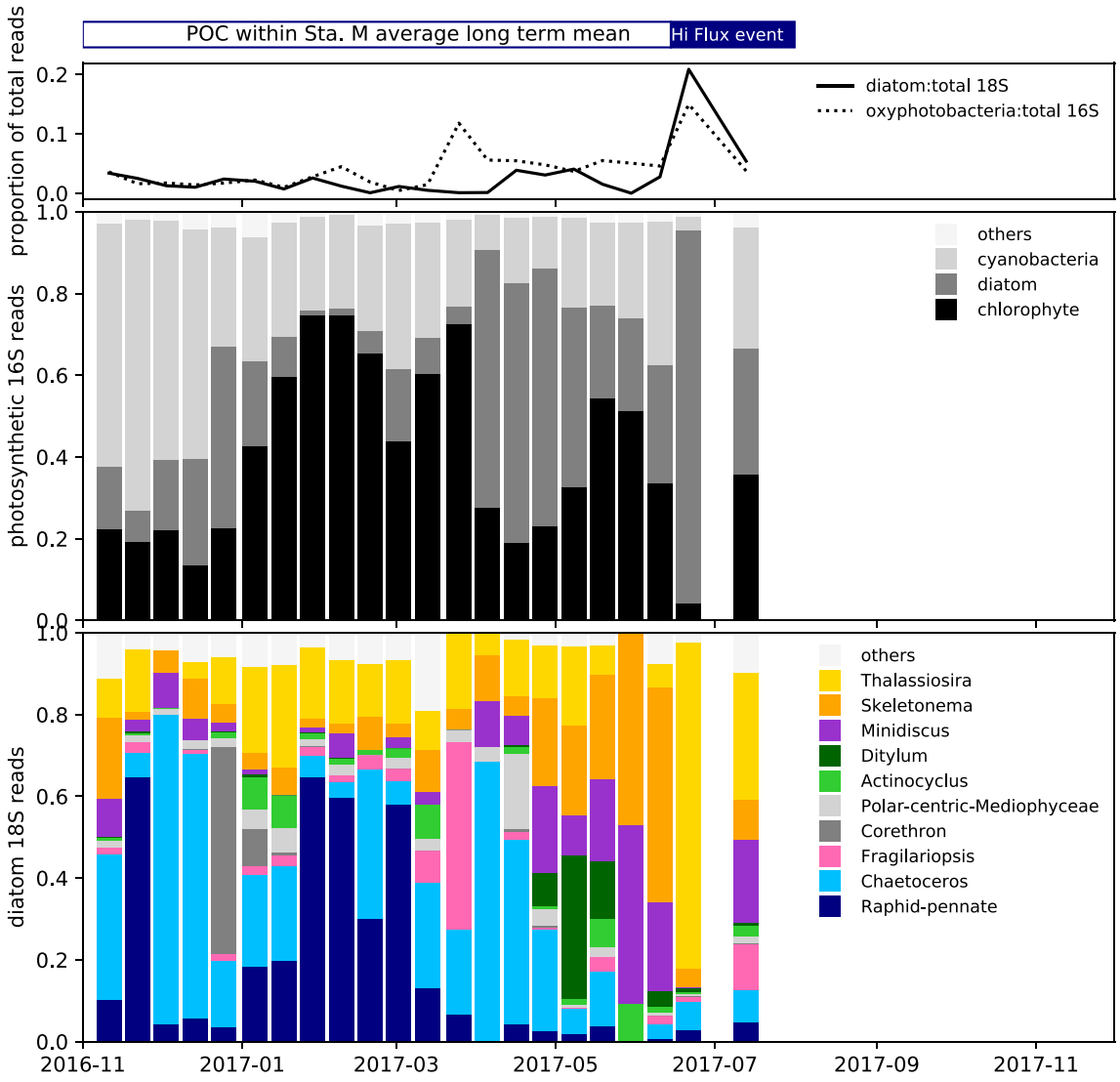

Fig. 4. Relative abundance (A) and taxonomic affiliation of 16S rRNA gene sequences belonging to oxyphotobacteria (B) and 18S rRNA gene sequences affiliated with Bacillariophyta (diatoms, C). 18S rRNA sequences belonging to land plants, chrysophytes, euglenoids, and coccolithophores were grouped into an "other" category due to their low (<1%) individual contributions to the total oxyphotobacteria dataset. All unassigned 16S rRNA gene sequences (7%) were excluded from analysis. Diatom genera contributing <1% of the relative abundance were grouped into the category "other". Timing of the high flux event is indicated by the blue bar at top.

bulk export process is not represented by water column samples (Amacher et al., 2013; Boeuf et al., 2019; Fontanez et al., 2015). We found similar results comparing the small subunit rRNA communities of two fractionated water column depth profiles collected within a few days of sinking POM collection in sediment traps. PERMANOVA, cluster analysis, and comparisons of common ASVs (100% identity) indicated different taxa comprising the community in both small subunit rRNAs of the >5 μm water column fraction, often considered the "particle attached" community, versus the sinking POM collected in sediment traps. Differences among the 16S rRNA gene libraries were more striking. The sample types shared few rRNA ASVs (100% identity) and groups indicative of bacterioplankton (SAR324, SAR406, SAR11, SUP05, planctomycetes, and archaea) rarely identified within the sinking POM collected in sediment traps compared to water column samples. Another indication that sinking particle communities were not well represented in samples from the water column was the absence of the Collodarian taxon in the water column that composed >95% of the sequences in the following sediment trap sample. This is likely due to patchy distribution of sinking particulates (McGill et al., 2016; Padilla et al., 2015) or organisms that form colonies (e.g. Collodarians, Stoecker et al., 2009), and the instantaneous sampling and limited sample volume (Padilla et al., 2015) collected by the Niskin bottles (5L) used here. In addition, whole water sampling collects all particulate types (sinking, buoyant and neutrally buoyant) compared to sediment traps that specifically target sinking POM. Thus, utilizing fractionated water column samples to predict the proportion or type of particulates that represent sinking POM is problematic.

Sea-floor aggregates collected here likely represent so called "dragon-king" particles, large and rare particulates that deviate from the normal size spectrum and likely provide unique habitats (Bochdansky et al., 2016). These large aggregates were enriched with benthic cercozoa and heterotrophic protists and contained a distinct community from sinking POM in sediment traps. Individual sea floor aggregates contained a large percentage of very rare ASVs (<0.003) and only shared a small percentage of common ASVs. These results may indicate variability in the degree to which samples were contaminated by surrounding seawater or sediment, and/or represent the variability of real changes in community composition (e.g. particles colonized by different organisms).

4.2. Sources and attenuation of sinking POM at station M

We relied on the sediment traps to provide a nearly continuous record of the organismal diversity of sinking POM (11-day integrated samples) reaching abyssal depths at Station M. Our results were similar in many ways to a study characterizing the sinking POM community at Station ALOHA (Boeuf et al., 2019), but also provided evidence of seasonality and organisms driving episodic high POC flux events in a coastally influenced environment. We also found the eukaryal community in the sinking POM to be much more variable and sporadic over time than the bacterial community (eight 18S rRNA clusters versus four 16S rRNA clusters, Figs. 1–3). The 16S rRNA clusters often did not change during sporadic and large inputs of radiolarian or metazoan taxa. Rather, the community change depended on the relative abundances of deep sea gammaproteobacteria and groups associated with phytoplankton blooms. At Station M, the particle communities changed over time, including the transition to spring conditions (beginning late March) and with the onset of a high POC flux event (June, Fig. 3). Changes in the eukaryotic community revealed which taxa were major contributors to attenuating the POM during those transitions (e.g. zooplankton, gelatinous filter feeders and heterotrophic protists). The 16S rRNA community provided a clearer indicator of changes between more-attenuated (processed) and faster sinking POM than the 18S rRNA gene community and 18S rRNA community was more informative as to the mechanism of export. Both rRNA data sets were important in determining the source of the POC. Below we highlight the potential role of organisms at Station M whose influence on POC flux is well established (e.g. diatoms, zooplankton), and also those organisms whose influence has more recently gained attention but are still poorly quantified (e.g. rhizaria, cyanobacteria, and chlorophytes).

4.2.1. Photosynthetic community and potential export process

The consistent presence of sequences associated with *Synechococcus*, chlorophytes, and diatoms over the time series, supports the growing evidence that these groups are influential contributors to the generation of exported POC that reaches abyssal depths (Agusti et al., 2015; Boeuf et al., 2019; Karl et al., 2012; Lomas and Moran, 2011; Sohrin et al., 2011; Tréguer et al., 2018). Although all three groups appeared to contribute to POM during average POC flux at Station M, diatoms were observed to have a greater effect during periods of increasing POC flux.

During winter when POC flux at Station M was low but within the time series average, more oligotrophic (cyanobacteria and rhizaria) communities dominated, with some contribution of diatoms and chlorophytes. The photoautotrophic community was at its lowest relative abundance during winter. Based on the high relative abundance of crustacean and cnidarian sequences, we infer that zooplankton grazers were influential in POC transport during this period by repackaging particles into dense fecal pellets while also attenuating POC flux in the water column. During this period, the 16S rRNA community (16S-3) contained some of the highest abundances of *Nitrococcales* (Methylophaga) and *Alteromonadales* (*Colwellia),* groups implicated in utilizing labile DOM released from the breakdown of sinking POM (Fontanez et al., 2015; McCarren et al., 2010), suggesting the POM is more processed. Thus, we hypothesize that winter fluxes were generated by low production, oligotrophic communities that are transported more slowly to abyssal depths and attenuated in the water column by microbial degradation and repeated cycling through pelagic heterotrophic food webs (e.g. grazing and filter feeding).

Diatoms were an important contributor to changes observed during increased POM and POC delivery to the sea floor. Relatively more diatom sequences in both the 18S and 16S rRNA datasets and a greater abundance of diatom genera typical of coastal blooms, such as *Skeletonema* and *Ditylum*, were present in early spring when particulates with fluorescence began to accumulate on the sea floor. During this period, greater abundances of heterotrophic protists including radiolarians were observed compared to metazoans. These data illustrate the potential importance of coastal blooms of diatoms fueling POM accumulation on the sea floor even during periods of POC flux within the long-term average.

Most striking was the major contribution of a single diatom species at the onset of the high POC flux event. A species closely related to *Thalassiosira aestivalis,* not detected earlier in the time series, appeared to be the producer of the POC that was exported from the euphotic zone to sea floor rapidly (~10 days, Smith et al., 2018) and lead to >99% coverage of the sea floor. As the flux event continued, a more mixed community of autotrophs was observed. The 16S rRNA particulate community during this period was quite different than previous samples and contained many bacterioplankton taxa often associated with phytoplankton blooms (SAR116, *Roseobacter* NAC11-7, OM27, OM43, OM60 (NOR5), and SAR86). This indicates injection of larger, faster sinking diatom-rich particulates which corroborates evidence that this event reached abyssal depths within days (Smith et al., 2018). In addition, the relative abundance of metazoan, copepod and cnidaria sequences also increased, and we hypothesize that these organisms grazed upon and repackaged the bloom community into fast sinking fecal pellets, efficiently transporting large quantities of relatively fresh POC to the deep ocean.

4.2.2. Influence of heterotrophic protists

Like other studies (Amacher et al., 2009; Boeuf et al., 2019; Fontanez et al., 2015), sequences belonging to heterotrophic protists dominated the library. Most heterotrophic protists were consistently present, showing some changes in relative abundance among sample clusters or across seasons. For example, heterotrophic and parasitic protists (Radiolaria, Dinoflagellatea, Apicomplexa, Excavata, and Oomycota) were consistent contributors to POC degradation of sinking particles regardless of season or particle composition. In particular, radiolarians at times dominated the 18S rRNA sequences and were represented by diverse radiolarian orders (see below). The consistent and dominant presence of diverse groups of heterotrophic protists reflects their importance on attenuating particles reaching abyssal depths.

During the 9-month sediment trap deployment, diverse radiolarian orders Acantharea, Polycystinea, Collodaria, RAD-A, RAD-B, RAD-C were present accounting for 5–99% of the sequences in samples over the time series. Two orders, RAD-A and Chaunacanthida were present in every single sediment trap sample (Table 3) and two Polycystinea radiolarians, Collodaria and Spumellarida, accounted for more than 50% of the sequences (Fig. 1) for 60 days of the 220-day time series. These orders were found within sinking POM in an upper water column study in the California current (Gutierrez-Rodriguez et al., 2019), thus our finding of highly variable radiolarian taxa exported to abyssal depths is not surprising.

Despite their consistent presence, periods where radiolarians dominated did not correspond with increasing POC flux or an accumulation of aggregates on the sea floor. The apparent dominance of radiolarians in the particle community is likely inflated by the large quantities of DNA encoded in each cell (Biard et al., 2017), biasing their apparent influence on overall particle quantity or quality. Our data suggest that radiolaria play a key role in the ecological dynamics of sinking particles, but do not provide evidence for driving large changes in the magnitude or quality of POC flux to the sea floor. This is in contrast to a study in the Northeast Atlantic (Lampitt et al., 2009) implicating radiolarians as the driver of high flux events.

Some Collodaria, Spumellarida, and Acantharia are known to harbor photosynthetic symbionts (Biard et al., 2016; Decelle et al., 2013; Stoecker et al., 2009) as well as parasites (Bråte et al., 2012). The majority of chloroplast sequences affiliated with chlorophytes were represented by a single ASV, present in every single sediment trap sample collected (Table 2). Interestingly, its highest relative abundance was observed March 25-April 15 when the Collodaria were most abundant (>95% sequences), though we acknowledge that ecological relationships other than symbiosis could also be responsible for this correspondence. If carrying autotrophic symbionts, radiolarian fluxes could

be an important export source of freshly generated organic matter to the sea floor during otherwise low POC flux periods.

4.2.3. Methodological considerations

It is critical to appreciate the strengths and biases of this molecular approach to accurately interpret results. This approach cannot detect the influence of phytoplankton whose DNA was degraded but whose organic material remains. Moreover, known PCR amplification biases and primer mismatches prevent the detection of some taxa (Apprill et al., 2015; Caron and Hu, 2019). For example in this study, coccolithophore sequences were detected in such low abundance that they did not qualify as a quantifiable group by our statistical standards, but they are observed by microscopy in high abundance (CAD, personal observation). In contrast, dinoflagellate sequences were relatively abundant in most trap samples even though they are typically not abundant when quantified by microscopy (CAD personal observation and Durkin et al., 2016). This mismatch is likely caused by the high ribosomal copy numbers per cell in dinoflagellates (Lin, 2011) and poor preservation of intact cells, two biases that also affect radiolarian taxa (Biard et al., 2017). Lastly, the ecological importance of taxa with low sequence abundance may be underappreciated. For example, some taxa (e.g. Nanomia and Ctenophora) although low in sequence abundance persisted for a long time (during winter, ~131 days) and thus they may have an appreciable impact on repackaging POM as it sinks to abyssal depths if integrated over time. In spite of these biases, molecular tools enable us to detect the influence of organisms that are difficult to observe by microscopy, such as collodarians, chlorophytes, bacteria, archaea and degraded cells.

5. Conclusions

Together these observations of particles at abyssal depths support long standing paradigms of plankton and particle dynamics that determine POC flux at the sea floor and further resolve biological details that help explain mechanisms of export. Episodic POC flux events at Station M have been increasing during the last decade, which implies that the processes controlling carbon flux are changing (Smith et al., 2013, 2018). These data from the onset of a single high flux event indicate that export of relatively unprocessed POC from diatom blooms, potentially transported within zooplankton fecal pellets, may be one mechanism driving these long-term changes. More frequent export of coastal diatom blooms at Station M could be driven by offshore transport by coastal jets or meanders in the California Current (Barth et al., 2002; Stukel et al., 2018b, 2017); physical processes driven by large scale climate dynamics. Observed increases in coastal production (Kahru et al., 2009) could also drive increasing POC export. Integrating biologically-resolved observations like these into the long-term monitoring of sinking particles is needed to determine the biological drivers of changing POC export into the deep ocean.

Data accessibility

The raw data supporting the conclusions will be made available by the authors. The 18S and 16S ribosomal rRNA amplicon sequence data sets were deposited into the NCBI Sequence Read Archive (BioProject number PRJNA591905).

Declaration of competing interest

The authors declare that they have no known competing financial interests or personal relationships that could have appeared to influence the work reported in this paper.

CRediT authorship contribution statement

Christina M. Preston: Conceptualization, Investigation, Formal analysis, Writing - original draft, Writing - review & editing. **Colleen A. Durkin:** Conceptualization, Investigation, Writing - original draft, Writing - review & editing. **Kevan M. Yamahara:** Writing - review & editing.

Acknowledgements

We thank Ken Smith Jr. and Christina Huffard for providing the POC data, ROVER data, and collecting sediment trap and water column samples used in this study. We like to thank the Captain and Crews of the R/V Western Flyer and ROV Doc Ricketts. We also thank two anonymous reviewers for their comments. This work was supported by funds from the David and Lucille Packard Foundation and funds from California Sea Grant awarded to CAD (R/HCME-37).

Appendix A. Supplementary data

Supplementary data to this article can be found online at https://doi.org/10.1016/j.dsr2.2019.104708.

References

Agusti, S., González-Gordillo, J.I., Vaqué, D., Estrada, M., Cerezo, M.I., Salazar, G., Gasol, J.M., Duarte, C.M., 2015. Ubiquitous healthy diatoms in the deep sea confirm deep carbon injection by the biological pump. Nat. Commun. 6, 7608. https://doi.org/10.1038/ncomms8608.

Alldredge, A.L., Silver, M.W., 1988. Characteristics, dynamics and significance of marine snow. Prog. Oceanogr. https://doi.org/10.1016/0079-6611(88)90053-5.

Amacher, J., Neuer, S., Anderson, I., Massana, R., 2009. Molecular Approach to Determine Contributions of the Protist Community to Particle Flux, vol. 56, pp. 2206–2215.

Amacher, J., Neuer, S., Lomas, M., 2013. DNA-based molecular fingerprinting of eukaryotic protists and cyanobacteria contributing to sinking particle flux at the Bermuda Atlantic time-series study. Deep. Res. Part II Top. Stud. Oceanogr. 93, 71–83. https://doi.org/10.1016/j.dsr2.2013.01.001.

Anderson, M.J., 2001. A new method for non-parametric multivariate analysis of variance. Austral Ecol. 26, 32–46. https://doi.org/10.1111/j.1442-9993.2001.01070.pp.x.

Apprill, A., McNally, S., Parsons, R., Weber, L., 2015. Minor revision to V4 region SSU rRNA 806R gene primer greatly increases detection of SAR11 bacterioplankton. Aquat. Microb. Ecol. 75, 129–137.

Barth, J.A., Cowles, T.J., Kosro, P.M., Shearman, R.K., Huyer, A., Smith, R.L., 2002. Injection of carbon from the shelf to offshore beneath the euphotic zone in the California Current. J. Geophys. Res. Ocean. 107, 10–18. https://doi.org/10.1029/2001JC000956.

Beaulieu, S.E., Smith, K.L., 1998. Phytodetritus entering the benthic boundary layer and aggregated on the sea floor in the abyssal NE Pacific: macro- and microscopic composition. Deep Sea Res. Part II Top. Stud. Oceanogr. 45, 781–815. https://doi.org/10.1016/S0967-0645(98)00003-4.

Belcher, A., Henson, S.A., Manno, C., Hill, S.L., Atkinson, A., Thorpe, S.E., Fretwell, P., Ireland, L., Tarling, G.A., 2019. Krill faecal pellets drive hidden pulses of particulate organic carbon in the marginal ice zone. Nat. Commun. 10, 889. https://doi.org/10.1038/s41467-019-08847-1.

Biard, T., Bigeard, E., Audic, S., Poulain, J., Gutierrez-Rodriguez, A., Pesant, S., Stemmann, L., Not, F., 2017. Biogeography and diversity of Collodaria (Radiolaria) in the global ocean. ISME J. 11, 1331–1344. https://doi.org/10.1038/ismej.2017.12.

Biard, T., Stemmann, L., Picheral, M., Mayot, N., Vandromme, P., Hauss, H., Gorsky, G., Guidi, L., Kiko, R., Not, F., 2016. In situ imaging reveals the biomass of giant protists in the global ocean. Nature 532, 504–507. https://doi.org/10.1038/nature17652.

Bochdansky, A.B., Clouse, M.A., Herndl, G.J., 2016. Dragon kings of the deep sea: marine particles deviate markedly from the common number-size spectrum. Sci. Rep. 6, 22633.

Boeuf, D., Edwards, B.R., Eppley, J.M., Hu, S.K., Poff, K.E., Romano, A.E., Caron, D.A., Karl, D.M., DeLong, E.F., 2019. Biological composition and microbial dynamics of sinking particulate organic matter at abyssal depths in the oligotrophic open ocean. Proc. Natl. Acad. Sci. U. S. A 116, 11824–11832. https://doi.org/10.1073/pnas.1903080116.

Bokulich, N.A., Kaehler, B.D., Rideout, J.R., Dillon, M., Bolyen, E., Knight, R., Huttley, G. A., Caporaso, J.G., 2018. Optimizing taxonomic classification of marker-gene amplicon sequences with QIIME 2's q2-feature-classifier plugin. Microbiome 6, 90. https://doi.org/10.1186/s40168-018-0470-z.

Bolyen, E., Rideout, J.R., Dillon, M.R., Bokulich, N.A., Abnet, C.C., Al-Ghalith, G.A., Alexander, H., Alm, E.J., Arumugam, M., Asnicar, F., Bai, Y., Bisanz, J.E., Bittinger, K., Brejnrod, A., Brislawn, C.J., Brown, C.T., Callahan, B.J., Caraballo-Rodríguez, A.M., Chase, J., Cope, E.K., Da Silva, R., Diener, C., Dorrestein, P.C., Douglas, G.M., Durall, D.M., Duvallet, C., Edwardson, C.F., Ernst, M., Estaki, M., Fouquier, J., Gauglitz, J.M., Gibbons, S.M., Gibson, D.L., Gonzalez, A., Gorlick, K., Guo, J., Hillmann, B., Holmes, S., Holste, H., Huttenhower, C., Huttley, G.A.,

Janssen, S., Jarmusch, A.K., Jiang, L., Kaehler, B.D., Kang, K. Bin, Keefe, C.R., Keim, P., Kelley, S.T., Knights, D., Koester, I., Kosciolek, T., Kreps, J., Langille, M.G. I., Lee, J., Ley, R., Liu, Y.-X., Loftfield, E., Lozupone, C., Maher, M., Marotz, C., Martin, B.D., McDonald, D., McIver, L.J., Melnik, A.V., Metcalf, J.L., Morgan, S.C., Morton, J.T., Naimey, A.T., Navas-Molina, J.A., Nothias, L.F., Orchanian, S.B., Pearson, T., Peoples, S.L., Petras, D., Preuss, M.L., Pruesse, E., Rasmussen, L.B., Rivers, A., Robeson, M.S., Rosenthal, P., Segata, N., Shaffer, M., Shiffer, A., Sinha, R., Song, S.J., Spear, J.R., Swafford, A.D., Thompson, L.R., Torres, P.J., Trinh, P., Tripathi, A., Turnbaugh, P.J., Ul-Hasan, S., van der Hooft, J.J.J., Vargas, F., Vázquez-Baeza, Y., Vogtmann, E., von Hippel, M., Walters, W., Wan, Y., Wang, M., Warren, J., Weber, K.C., Williamson, C.H.D., Willis, A.D., Xu, Z.Z., Zaneveld, J.R., Zhang, Y., Zhu, Q., Knight, R., Caporaso, J.G., 2019. Reproducible, interactive, scalable and extensible microbiome data science using QIIME 2. Nat. Biotechnol. 37, 852–857. https://doi.org/10.1038/s41587-019-0209-9.

Boratyn, G.M., Camacho, C., Cooper, P.S., Coulouris, G., Fong, A., Ma, N., Madden, T.L., Matten, W.T., McGinnis, S.D., Merezhuk, Y., Raytselis, Y., Sayers, E.W., Tao, T., Ye, J., Zaretskaya, I., 2013. BLAST: a more efficient report with usability improvements. Nucleic Acids Res. 41, W29–W33. https://doi.org/10.1093/nar/gkt282.

Bråte, J., Krabberød, A.K., Dolven, J.K., Ose, R.F., Kristensen, T., Bjørklund, K.R., Shalchian-Tabrizi, K., 2012. Radiolaria associated with large diversity of marine alveolates. Protist 163, 767–777. https://doi.org/10.1016/j.protis.2012.04.004.

Buesseler, K.O., Trull, T.W., Steinberg, D.K., Silver, M.W., Siegel, D.A., Saitoh, S.-I., Lamborg, C.H., Lam, P.J., Karl, D.M., Jiao, N.Z., Honda, M.C., Elskens, M., Dehairs, F., Brown, S.L., Boyd, P.W., Bishop, J.K.B., Bidigare, R.R., 2008. VERTIGO (VERtical Transport in the Global Ocean): a study of particle sources and flux attenuation in the North Pacific. Deep Sea Res. Part II Top. Stud. Oceanogr. 55, 1522–1539. https://doi.org/10.1016/J.DSR2.2008.04.024.

Callahan, B.J., McMurdie, P.J., Rosen, M.J., Han, A.W., Johnson, A.J.A., Holmes, S.P., 2016. DADA2: high-resolution sample inference from Illumina amplicon data. Nat. Methods 13, 581.

Caron, D.A., Hu, S.K., 2019. Are we overestimating protistan diversity in nature? Trends Microbiol. https://doi.org/10.1016/j.tim.2018.10.009.

Caron, D.A., Madin, L.P., Cole, J.J., 1989. Composition and degradation of salp fecal pellets: implications for vertical flux in oceanic environments. J. Mar. Res. 47, 829–850.

Cho, B.C., Azam, F., 1988. Major role of bacteria in biogeochemical fluxes in the ocean's interior. Nature 332, 441–443. https://doi.org/10.1038/332441a0.

Conte, M.H., Ralph, N., Ross, E.H., 2001. Seasonal and interannual variability in deep ocean particle fluxes at the Oceanic Flux Program (OFP)/Bermuda Atlantic Time Series (BATS) site in the western Sargasso Sea near Bermuda. Deep. Res. Part II Top. Stud. Oceanogr. 48, 1471–1505. https://doi.org/10.1016/S0967-0645(00)00150-8.

De La Rocha, C.L., Passow, U., 2007. Factors influencing the sinking of POC and the efficiency of the biological carbon pump. Deep. Res. Part II Top. Stud. Oceanogr. 54, 639–658. https://doi.org/10.1016/j.dsr2.2007.01.004.

De Wit, P., Pespeni, M.H., Ladner, J.T., Barshis, D.J., Seneca, F., Jaris, H., Therkildsen, N. O., Morikawa, M., Palumbi, S.R., 2012. The simple fool's guide to population genomics via RNA-Seq: an introduction to high-throughput sequencing data analysis. Mol. Ecol. Resour. 12, 1058–1067. https://doi.org/10.1111/1755-0998.12003.

Decelle, J., Martin, P., Paborstava, K., Pond, D.W., Tarling, G., Mahé, F., de Vargas, C., Lampitt, R., Not, F., 2013. Diversity, ecology and biogeochemistry of cyst-forming Acantharia (radiolaria) in the oceans. PLoS One 8, 1–13. https://doi.org/10.1371/journal.pone.0053598.

DeLong, E.F., Franks, D.G., Alldredge, A.L., 1993. Phylogenetic diversity of aggregate-attached vs. free-living marine bacterial assemblages. Limnol. Oceanogr. 38, 924–934. https://doi.org/10.4319/lo.1993.38.5.0924.

Ducklow, H.W., Steinberg, D.K., Buesseler, K.O., 2001. Upper Ocean carbon export and the biological pump. Oceanography 14, 50–58.

Durkin, C.A., Van Mooy, B.A.S., Dyhrman, S.T., Buesseler, K.O., 2016. Sinking phytoplankton associated with carbon flux in the Atlantic Ocean. Limnol. Oceanogr. 61, 1172–1187. https://doi.org/10.1002/lno.10253.

Ebersbach, F., Assmy, P., Martin, P., Schulz, I., Wolzenburg, S., Nöthig, E.M., 2014. Particle flux characterisation and sedimentation patterns of protistan plankton during the iron fertilisation experiment LOHAFEX in the Southern Ocean. Deep. Res. Part I Oceanogr. Res. Pap. 89, 94–103. https://doi.org/10.1016/j.dsr.2014.04.007.

Eloe, E.A., Shulse, C.N., Fadrosh, D.W., Williamson, S.J., Allen, E.E., Bartlett, D.H., 2011. Compositional differences in particle-associated and free-living microbial assemblages from an extreme deep-ocean environment. Environ. Microbiol. Rep. 3, 449–458. https://doi.org/10.1111/j.1758-2229.2010.00223.x.

Faith, D.P., Minchin, P.R., Belbin, L., 1987. Compositional dissimilarity as a robust measure of ecological distance. Vegetatio 69, 57–68. https://doi.org/10.1007/BF00038687.

Fontanez, K.M., Eppley, J.M., Samo, T.J., Karl, D.M., DeLong, E.F., 2015. Microbial community structure and function on sinking particles in the North Pacific Subtropical Gyre. Front. Microbiol. 6, 469. https://doi.org/10.3389/fmicb.2015.00469.

Francois, R., Honjo, S., Krishfield, R., Manganini, S., 2002. Factors controlling the flux of organic carbon to the bathypelagic zone of the ocean. Glob. Biogeochem. Cycles 16, 34-1-34–20.

Ganesh, S., Parris, D.J., DeLong, E.F., Stewart, F.J., 2013. Metagenomic analysis of size-fractionated picoplankton in a marine oxygen minimum zone. ISME J. 8, 187.

Guidi, L., Chaffron, S., Bittner, L., Eveillard, D., Larhlimi, A., Roux, S., Darzi, Y., Audic, S., Berline, L., Brum, J.R., Coelho, L.P., Espinoza, J.C.I., Malviya, S., Sunagawa, S., Dimier, C., Kandels-Lewis, S., Picheral, M., Poulain, J., Searson, S., Stemmann, L., Not, F., Hingamp, P., Speich, S., Follows, M., Karp-Boss, L., Boss, E., Ogata, H., Pesant, S., Weissenbach, J., Wincker, P., Acinas, S.G., Bork, P., De Vargas, C., Iudicone, D., Sullivan, M.B., Raes, J., Karsenti, E., Bowler, C., Gorsky, G., 2016. Plankton networks driving carbon export in the oligotrophic ocean. Nature 532, 465–470. https://doi.org/10.1038/nature16942.

Guillou, L., Bachar, D., Audic, S., Bass, D., Berney, C., Bittner, L., Boutte, C., Burgaud, G., de Vargas, C., Decelle, J., del Campo, J., Dolan, J.R., Dunthorn, M., Edvardsen, B., Holzmann, M., Kooistra, W.H.C.F., Lara, E., Le Bescot, N., Logares, R., Mahé, F., Massana, R., Montresor, M., Morard, R., Not, F., Pawlowski, J., Probert, I., Sauvadet, A.-L., Siano, R., Stoeck, T., Vaulot, D., Zimmermann, P., Christen, R., 2012. The Protist Ribosomal Reference database (PR2): a catalog of unicellular eukaryote Small Sub-Unit rRNA sequences with curated taxonomy. Nucleic Acids Res. 41, D597–D604. https://doi.org/10.1093/nar/gks1160.

Gutierrez-Rodriguez, A., Stukel, M.R., Lopes dos Santos, A., Biard, T., Scharek, R., Vaulot, D., Landry, M.R., Not, F., 2019. High contribution of Rhizaria (Radiolaria) to vertical export in the California Current Ecosystem revealed by DNA metabarcoding. ISME J. 13, 964–976. https://doi.org/10.1038/s41396-018-0322-7.

Hansen, J., Kiorboe, T., AL, A., 1996. Marine snow derived from abandoned larvacean houses: sinking rates, particle content and mechanisms of aggregate formation. Mar. Ecol. Prog. Ser. 141, 205–215.

Henson, S., Sanders, R., Madsen, E., 2012. Global patterns in efficiency of particulate organic carbon export and transfer to the deep ocean. Glob. Biogeochem. Cycles 26, GB1028.

Herndl, G.J., Reinthaler, T., 2013. Microbial control of the dark end of the biological pump. Nat. Geosci. 6, 718–724. https://doi.org/10.1038/ngeo1921.

Kahru, M., Kudela, R., Manzano-Sarabia, M., Mitchell, B.G., 2009. Trends in primary production in the California Current detected with satellite data. J. Geophys. Res. Ocean. 114 https://doi.org/10.1029/2008JC004979.

Karl, D.M., Church, M.J., Dore, J.E., Letelier, R.M., Mahaffey, C., 2012. Predictable and efficient carbon sequestration in the North Pacific Ocean supported by symbiotic nitrogen fixation. Proc. Natl. Acad. Sci. U. S. A 109, 1842–1849. https://doi.org/10.1073/pnas.1120312109.

Katija, K., Sherlock, R.E., Sherman, A.D., Robison, B.H., 2017. New technology reveals the role of giant larvaceans in oceanic carbon cycling. Sci. Adv. 3, e1602374 https://doi.org/10.1126/sciadv.1602374.

Katoh, K., Standley, D.M., 2013. MAFFT multiple sequence alignment software version 7: improvements in performance and usability. Mol. Biol. Evol. 30, 772–780. https://doi.org/10.1093/molbev/mst010.

Kembel, S.W., Wu, M., Eisen, J.A., Green, J.L., 2012. Incorporating 16S gene copy number information improves estimates of microbial diversity and abundance. PLoS Comput. Biol. 8, e1002743.

Lampitt, R., Salter, I., de Cuevas, B.A., Hartman, S., Larkin, K.E., Pebody, C.A., 2010. Long-term variability of downward particle flux in the deep northeast Atlantic: causes and trends. Deep Sea Res. Part II Top. Stud. Oceanogr. 57, 1346–1361. https://doi.org/10.1016/J.DSR2.2010.01.011.

Lampitt, R.S., 1992. The contribution of deep-sea macroplankton to organic remineralization: results from sediment trap and zooplankton studies over the Madeira Abyssal Plain. Deep Sea Res. Part A, Oceanogr. Res. Pap. 39, 221–233. https://doi.org/10.1016/0198-0149(92)90106-4.

Lampitt, R.S., Salter, I., Johns, D., 2009. Radiolaria: major exporters of organic carbon to the deep ocean. Glob. Biogeochem. Cycles 23. https://doi.org/10.1029/2008GB003221 n/a-n/a.

Lebrato, M., Benavides, R., Oschlies, A., de Jesus Mendes, P., Steinberg, D.K., Cartes, J.E., Jones, B.M., Birsa, L.M., 2013. Jelly biomass sinking speed reveals a fast carbon export mechanism. Limnol. Oceanogr. 58, 1113–1122. https://doi.org/10.4319/lo.2013.58.3.1113.

Lin, S., 2011. Genomic understanding of dinoflagellates. Res. Microbiol. 162, 551–569. https://doi.org/10.1016/j.resmic.2011.04.006.

Liu, R., Wang, L., Liu, Q., Wang, Z., Li, Z., Fang, J., Zhang, L., Luo, M., 2018. Depth-resolved distribution of particle-attached and free-living bacterial communities in the water column of the new britain trench. Front. Microbiol. 9, 625. https://doi.org/10.3389/fmicb.2018.00625.

Lomas, M.W., Moran, S.B., 2011. Evidence for aggregation and export of cyanobacteria and nano-eukaryotes from the Sargasso Sea euphotic zone. Biogeosciences 8, 203–216. https://doi.org/10.5194/bg-8-203-2011.

Mantel, N., 1967. The detection of disease clustering and a generalized regression approach. Cancer Res. 27, 209–220.

McCarren, J., Becker, J.W., Repeta, D.J., Shi, Y., Young, C.R., Malmstrom, R.R., Chisholm, S.W., DeLong, E.F., 2010. Microbial community transcriptomes reveal microbes and metabolic pathways associated with dissolved organic matter turnover in the sea. Proc. Natl. Acad. Sci. 107 https://doi.org/10.1073/pnas.1010732107, 16420 LP – 16427.

McDonald, D., Clemente, J.C., Kuczynski, J., Rideout, J.R., Stombaugh, J., Wendel, D., Wilke, A., Huse, S., Hufnagle, J., Meyer, F., Knight, R., Caporaso, J.G., 2012. The Biological Observation Matrix (BIOM) format or: how I learned to stop worrying and love the ome-ome. GigaScience 1, 7. https://doi.org/10.1186/2047-217X-1-7.

McGill, P.R., Henthorn, R.G., Bird, L.E., Huffard, C.L., Klimov, D.V., Smith Jr., K.L., 2016. Sedimentation event sensor: new ocean instrument for in situ imaging and fluorometry of sinking particulate matter. Limnol Oceanogr. Methods 14, 853–863. https://doi.org/10.1002/lom3.10131.

McKinney, W., 2010. Data structures for statistical computing in Python. In: van der Walt, S., Millman, J. (Eds.), Proceedings of the 9th Python in Science Conference, pp. 51–56.

Mestre, M., Ruiz-González, C., Logares, R., Duarte, C.M., Gasol, J.M., Sala, M.M., 2018. Sinking particles promote vertical connectivity in the ocean microbiome. Proc. Natl. Acad. Sci. 115 https://doi.org/10.1073/pnas.1802470115. E6799 LP-E6807.

Nagata, T., Tamburini, C., Arístegui, J., Baltar, F., Bochdansky, A.B., Fonda-Umani, S., Fukuda, H., Gogou, A., Hansell, D.A., Hansman, R.L., Herndl, G.J.,

Panagiotopoulos, C., Reinthaler, T., Sohrin, R., Verdugo, P., Yamada, N., Yamashita, Y., Yokokawa, T., Bartlett, D.H., 2010. Emerging concepts on microbial processes in the bathypelagic ocean - ecology, biogeochemistry, and genomics. Deep. Res. Part II Top. Stud. Oceanogr. 57, 1519–1536. https://doi.org/10.1016/j.dsr2.2010.02.019.

Padilla, C.C., Ganesh, S., Gantt, S., Huhman, A., Parris, D.J., Sarode, N., Stewart, F.J., 2015. Standard filtration practices may significantly distort planktonic microbial diversity estimates. Front. Microbiol. 6, 547. https://doi.org/10.3389/fmicb.2015.00547.

Parada, A.E., Needham, D.M., Fuhrman, J.A., 2016. Every base matters: assessing small subunit rRNA primers for marine microbiomes with mock communities, time series and global field samples. Environ. Microbiol. 18, 1403–1414. https://doi.org/10.1111/1462-2920.13023.

Pearson, K., 1895. Note on regression and inheritance in the case of two parents. Proc. R. Soc. Lond. 58, 240–242.

Peoples, L.M., Donaldson, S., Osuntokun, O., Xia, Q., Nelson, A., Blanton, J., Allen, E.E., Church, M.J., Bartlett, D.H., 2018. Vertically distinct microbial communities in the mariana and kermadec trenches. PLoS One 13, e0195102. https://doi.org/10.1371/journal.pone.0195102.

Price, M.N., Dehal, P.S., Arkin, A.P., 2010. FastTree 2–approximately maximum-likelihood trees for large alignments. PLoS One 5. https://doi.org/10.1371/journal.pone.0009490 e9490.

Quast, C., Pruesse, E., Yilmaz, P., Gerken, J., Schweer, T., Yarza, P., Peplies, J., Glöckner, F.O., 2012. The SILVA ribosomal RNA gene database project: improved data processing and web-based tools. Nucleic Acids Res. 41, D590–D596. https://doi.org/10.1093/nar/gks1219.

Riley, J.S., Sanders, R., Marsay, C., Le Moigne, F.A.C., Achterberg, E.P., Poulton, A.J., 2012. The relative contribution of fast and slow sinking particles to ocean carbon export. Glob. Biogeochem. Cycles 26. https://doi.org/10.1029/2011GB004085. GB1026.

Robison, B., Reisenbichler, K., Sherlock, R., 2005. Giant larvacean houses: rapid carbon transport to the deep sea floor. Science (80-.) 308, 1609–1611. https://doi.org/10.1126/science.1109104.

Rynearson, T.A., Richardson, K., Lampitt, R.S., Sieracki, M.E., Poulton, A.J., Lyngsgaard, M.M., Perry, M.J., 2013. Major contribution of diatom resting spores to vertical flux in the sub-polar North Atlantic. Deep. Res. Part I Oceanogr. Res. Pap. 82, 60–71. https://doi.org/10.1016/j.dsr.2013.07.013.

Schnetzer, A., 2002. Active transport of particulate organic carbon and nitrogen by vertically migrating zooplankton in the Sargasso Sea. Mar. Ecol. Prog. Ser. 234, 71–84.

Sherman, A.D., Smith, K.L., 2009. Deep-sea benthic boundary layer communities and food supply: a long-term monitoring strategy. Deep Sea Res. Part II Top. Stud. Oceanogr. 56, 1754–1762. https://doi.org/10.1016/J.DSR2.2009.05.020.

Silver, M.W., Bruland, K.W., 1981. Differential feeding and fecal pellet composition of salps and pteropods, and the possible origin of the deep-water flora and olive-green "Cells". Mar. Biol. 62, 263–273. https://doi.org/10.1007/BF00397693.

Silver, M.W., Gowing, M.M., 1991. The "particle" flux: origins and biological components. Prog. Oceanogr. https://doi.org/10.1016/0079-6611(91)90007-9.

Smith, D.C., Simon, M., Alldredge, A.L., Azam, F., 1992. Intense hydrolytic enzyme activity on marine aggregates and implications for rapid particle dissolution. Nature 359, 139–142. https://doi.org/10.1038/359139a0.

Smith, K., Ruhl, H., Kahru, M., Huffard, C., Sherman, A., 2013. Deep ocean communities impacted by changing climate over 24 y in the abyssal northeast Pacific Ocean. Proc. Natl. Acad. Sci. U.S.A. 110, 19838–19841. https://doi.org/10.1073/pnas.1315447110.

Smith, K.L., Baldwin, R.J., Ruhl, H.A., Kahru, M., Mitchell, B.G., Kaufmann, R.S., 2006. Climate effect on food supply to depths greater than 4,000 meters in the northeast Pacific. Limnol. Oceanogr. 51, 166–176. https://doi.org/10.4319/lo.2006.51.1.0166.

Smith, K.L., Druffel, E.R.M., 1998. Long time-series monitoring of an abyssal site in the NE Pacific: an introduction. Deep. Res. Part II Top. Stud. Oceanogr. 45, 573–586. https://doi.org/10.1016/S0967-0645(97)00094-5.

Smith, K.L., Ruhl, H.A., Huffard, C.L., Messié, M., Kahru, M., 2018. Episodic organic carbon fluxes from surface ocean to abyssal depths during long-term monitoring in NE Pacific. Proc. Natl. Acad. Sci. U. S. A 115, 12235–12240. https://doi.org/10.1073/pnas.1814559115.

Smith, K.L.J., Ruhl, H.A., Kaufmann, R.S., Kahru, M., 2008. Tracing abyssal food supply back to upper-ocean processes over a 17-year time series in the northeast Pacific. Limnol. Oceanogr. 53, 2655–2667. https://doi.org/10.4319/lo.2008.53.6.2655.

Smith, K.L.J., Sherman, A.D., Huffard, C.L., McGill, P.R., Henthorn, R., Von Thun, S., Ruhl, H.A., Kahru, M., Ohman, M.D., 2014. Large salp bloom export from the upper ocean and benthic community response in the abyssal northeast Pacific: day to week resolution. Limnol. Oceanogr. 59, 745–757. https://doi.org/10.4319/lo.2014.59.3.0745.

Sohrin, R., Isaji, M., Obara, Y., Agostini, S., Suzuki, Y., Hiroe, Y., Ichikawa, T., Hidaka, K., 2011. Distribution of Synechococcus in the dark ocean. Aquat. Microb. Ecol. 64, 1–14.

Spearman, C., 1904. The proof and measurement of association between two things. Am. J. Psychol. 15, 72–101.

Steinberg, D.K., Goldthwait, S.A., Hansell, D.A., 2002. Zooplankton vertical migration and the active transport of dissolved organic and inorganic nitrogen in the Sargasso Sea. Deep. Res. Part I Oceanogr. Res. Pap. 49, 1445–1461. https://doi.org/10.1016/S0967-0637(02)00037-7.

Steinberg, D.K., Landry, M.R., 2017. Zooplankton and the ocean carbon cycle. Ann. Rev. Mar. Sci. 9, 413–444. https://doi.org/10.1146/annurev-marine-010814-015924.

Steinberg, D.K., Lomas, M.W., Cope, J.S., 2012. Long-term increase in mesozooplankton biomass in the Sargasso Sea: linkage to climate and implications for food web dynamics and biogeochemical cycling. Global Biogeochem. https://doi.org/10.1029/2010GB004026. Cycles 26.

Stoecker, D., Johnso, M., DeVargas, C., Not, F., 2009. Acquired phototrophy in aquatic protists. Aquat. Microb. Ecol. 57, 279–310.

Stone, J., Steinberg, D., 2016. Salp contributions to vertical carbon flux in the Sargasso Sea. Deep Sea Res. Part I 113, 90–100.

Stukel, M.R., Aluwihare, L.I., Barbeau, K.A., Chekalyuk, A.M., Goericke, R., Miller, A.J., Ohman, M.D., Ruacho, A., Song, H., Stephens, B.M., Landry, M.R., 2017. Mesoscale ocean fronts enhance carbon export due to gravitational sinking and subduction. Proc. Natl. Acad. Sci. 114, 1252–1257. https://doi.org/10.1073/PNAS.1609435114.

Stukel, M.R., Biard, T., Krause, J., Ohman, M.D., 2018a. Large Phaeodaria in the twilight zone: their role in the carbon cycle. Limnol. Oceanogr. 63, 2579–2594. https://doi.org/10.1002/lno.10961.

Stukel, M.R., Song, H., Goericke, R., Miller, A.J., 2018b. The role of subduction and gravitational sinking in particle export, carbon sequestration, and the remineralization length scale in the California Current Ecosystem. Limnol. Oceanogr. 63, 363–383. https://doi.org/10.1002/lno.10636.

Thompson, L.R., Sanders, J.G., McDonald, D., Amir, A., Ladau, J., Locey, K.J., Prill, R.J., Tripathi, A., Gibbons, S.M., Ackermann, G., Navas-Molina, J.A., Janssen, S., Kopylova, E., Vázquez-Baeza, Y., González, A., Morton, J.T., Mirarab, S., Zech Xu, Z., Jiang, L., Haroon, M.F., Kanbar, J., Zhu, Q., Jin Song, S., Kosciolek, T., Bokulich, N. A., Lefler, J., Brislawn, C.J., Humphrey, G., Owens, S.M., Hampton-Marcell, J., Berg-Lyons, D., McKenzie, V., Fierer, N., Fuhrman, J.A., Clauset, A., Stevens, R.L., Shade, A., Pollard, K.S., Goodwin, K.D., Jansson, J.K., Gilbert, J.A., Knight, R., Consortium, T.E.M.P., Rivera, J.L.A., Al-Moosawi, L., Alverdy, J., Amato, K.R., Andras, J., Angenent, L.T., Antonopoulos, D.A., Apprill, A., Armitage, D., Ballantine, K., Bárta, J., Baum, J.K., Berry, A., Bhatnagar, A., Bhatnagar, M., Biddle, J.F., Bittner, L., Boldgiv, B., Bottos, E., Boyer, D.M., Braun, J., Brazelton, W., Brearley, F.Q., Campbell, A.H., Caporaso, J.G., Cardona, C., Carroll, J., Cary, S.C., Casper, B.B., Charles, T.C., Chu, H., Claar, D.C., Clark, R.G., Clayton, J.B., Clemente, J.C., Cochran, A., Coleman, M.L., Collins, G., Colwell, R.R., Contreras, M., Crary, B.B., Creer, S., Cristol, D.A., Crump, B.C., Cui, D., Daly, S.E., Davalos, L., Dawson, R.D., Defazio, J., Delsuc, F., Dionisi, H.M., Dominguez-Bello, M.G., Dowell, R., Dubinsky, E.A., Dunn, P.O., Ercolini, D., Espinoza, R.E., Ezenwa, V., Fenner, N., Findlay, H.S., Fleming, I.D., Fogliano, V., Forsman, A., Freeman, C., Friedman, E.S., Galindo, G., Garcia, L., Garcia-Amado, M.A., Garshelis, D., Gasser, R. B., Gerdts, G., Gibson, M.K., Gifford, I., Gill, R.T., Giray, T., Gittel, A., Golyshin, P., Gong, D., Grossart, H.-P., Guyton, K., Haig, S.-J., Hale, V., Hall, R.S., Hallam, S.J., Handley, K.M., Hasan, N.A., Haydon, S.R., Hickman, J.E., Hidalgo, G., Hofmockel, K. S., Hooker, J., Hulth, S., Hultman, J., Hyde, E., Ibáñez-Álamo, J.D., Jastrow, J.D., Jex, A.R., Johnson, L.S., Johnston, E.R., Joseph, S., Jurburg, S.D., Jurelevicius, D., Karlsson, A., Karlsson, R., Kauppinen, S., Kellogg, C.T.E., Kennedy, S.J., Kerkhof, L. J., King, G.M., Kling, G.W., Koehler, A.V., Krezalek, M., Kueneman, J., Lamendella, R., Landon, E.M., Lane-deGraaf, K., LaRoche, J., Larsen, P., Laverock, B., Lax, S., Lentino, M., Levin, I.I., Liancourt, P., Liang, W., Linz, A.M., Lipson, D.A., Liu, Y., Lladser, M.E., Lozada, M., Spirito, C.M., MacCormack, W.P., MacRae-Crerar, A., Magris, M., Martín-Platero, A.M., Martín-Vivaldi, M., Martínez, L.M., Martínez-Bueno, M., Marzinelli, E.M., Mason, O.U., Mayer, G.D., McDevitt-Irwin, J.M., McDonald, J.E., McGuire, K.L., McMahon, K.D., McMinds, R., Medina, M., Mendelson, J.R., Metcalf, J.L., Meyer, F., Michelangeli, F., Miller, K., Mills, D.A., Minich, J., Mocali, S., Moitinho-Silva, L., Moore, A., Morgan-Kiss, R.M., Munroe, P., Myrold, D., Neufeld, J.D., Ni, Y., Nicol, G.W., Nielsen, S., Nissimov, J.I., Niu, K., Nolan, M.J., Noyce, K., O'Brien, S.L., Okamoto, N., Orlando, L., Castellano, Y.O., Osuolale, O., Oswald, W., Parnell, J., Peralta-Sánchez, J.M., Petraitis, P., Pfister, C., Pilon-Smits, E., Piombino, P., Pointing, S.B., Pollock, F.J., Potter, C., Prithiviraj, B., Quince, C., Rani, A., Ranjan, R., Rao, S., Rees, A.P., Richardson, M., Riebesell, U., Robinson, C., Rockne, K.J., Rodriguezl, S.M., Rohwer, F., Roundstone, W., Safran, R.J., Sangwan, N., Sanz, V., Schrenk, M., Schrenzel, M.D., Scott, N.M., Seger, R.L., Seguin-Orlando, A., Seldin, L., Seyler, L.M., Shakhsheer, B., Sheets, G.M., Shen, C., Shi, Y., Shin, H., Shogan, B.D., Shutler, D., Siegel, J., Simmons, S., Sjöling, S., Smith, D.P., Soler, J.J., Sperling, M., Steinberg, P. D., Stephens, B., Stevens, M.A., Taghavi, S., Tai, V., Tait, K., Tan, C.L., Tas, N., Taylor, D.L., Thomas, T., Timling, I., Turner, B.L., Urich, T., Ursell, L.K., van der Lelie, D., Van Treuren, W., van Zwieten, L., Vargas-Robles, D., Thurber, R.V., Vitaglione, P., Walker, D.A., Walters, W.A., Wang, S., Wang, T., Weaver, T., Webster, N.S., Wehrle, B., Weisenhorn, P., Weiss, S., Werner, J.J., West, K., Whitehead, A., Whitehead, S.R., Whittingham, L.A., Willerslev, E., Williams, A.E., Wood, S.A., Woodhams, D.C., Yang, Y., Zaneveld, J., Zarraonaindia, I., Zhang, Q., Zhao, H., 2017. A communal catalogue reveals Earth's multiscale microbial diversity. Nature 551, 457.

Tréguer, P., Bowler, C., Moriceau, B., Dutkiewicz, S., Gehlen, M., Aumont, O., Bittner, L., Dugdale, R., Finkel, Z., Iudicone, D., Jahn, O., Guidi, L., Lasbleiz, M., Leblanc, K., Levy, M., Pondaven, P., 2018. Influence of diatom diversity on the ocean biological carbon pump. Nat. Geosci. 11, 27–37. https://doi.org/10.1038/s41561-017-0028-x.

Turner, J.T., 2015. Zooplankton fecal pellets, marine snow, phytodetritus and the ocean's biological pump. Prog. Oceanogr. https://doi.org/10.1016/j.pocean.2014.08.005.

Waite, A., Bienfang, P.K., Harrison, P.J., 1992. Spring bloom sedimentation in a subarctic ecosystem. Mar. Biol. 114, 131–138. https://doi.org/10.1007/BF00350862.

Weiss, S., Xu, Z.Z., Peddada, S., Amir, A., Bittinger, K., Gonzalez, A., Lozupone, C., Zaneveld, J.R., Vázquez-Baeza, Y., Birmingham, A., Hyde, E.R., Knight, R., 2017. Normalization and microbial differential abundance strategies depend upon data characteristics. Microbiome 5, 27. https://doi.org/10.1186/s40168-017-0237-y.

Wilson, S., Ruhl, H., Smith, K., 2013. Zooplankton fecal pellet flux in the abyssal northeast Pacific: a 15 year time-series study. Limnol. Oceanogr. 58, 881–892.
Wilson, S., Steinberg, D., 2010. Autotrophic picoplankton in mesozooplankton guts: evidence of aggregate feeding in the mesopelagic zone and export of small phytoplankton. Mar. Ecol. Prog. Ser. 412, 11–27.
Wong, C.S., Whitney, F.A., Crawford, D.W., Iseki, K., Matear, R.J., Johnson, W.K., Page, J.S., Timothy, D., 1999. Seasonal and interannual variability in particle fluxes of carbon, nitrogen and silicon from time series of sediment traps at Ocean Station P, 1982-1993: relationship to changes in subarctic primary productivity. Deep. Res. Part II Top. Stud. Oceanogr. 46, 2735–2760. https://doi.org/10.1016/S0967-0645(99)00082-X.
Xu, Z., Wang, M., Wu, W., Li, Y., Liu, Q., Han, Y., Jiang, Y., Shao, H., McMinn, A., Liu, H., 2018. Vertical distribution of microbial eukaryotes from surface to the hadal zone of the mariana trench. Front. Microbiol. 9, 2023. https://doi.org/10.3389/fmicb.2018.02023.